

Filling transition for a wedge

K. Rejmer ^{1,2}, S. Dietrich ¹, and M. Napiórkowski ²

¹ *Fachbereich Physik, Bergische Universität Wuppertal,
D-42097 Wuppertal, Germany*

² *Instytut Fizyki Teoretycznej, Uniwersytet Warszawski,
00-681 Warszawa, Hoża 69, Poland*

Abstract

We study the formation and the shape of a liquid meniscus in a wedge with opening angle 2φ which is exposed to a vapor phase. By applying a suitable effective interface model, at liquid-vapor coexistence and at a temperature T_φ we find a filling transition at which the height of the meniscus becomes macroscopically large while the planar walls of the wedge far away from its center remain nonwet up to the wetting transition occurring at $T_w > T_\varphi$. Depending on the fluid and the substrate potential the filling transition can be either continuous or discontinuous. In the latter case it is accompanied by a owprefilling line extending into the vapor phase of the bulk phase diagram and describing a transition from a small to a large, but finite, meniscus height. The filling and the prefilling transitions correspond to nonanalyticities in the surface and line contributions to the free energy of the fluid, respectively.

PACS numbers : 68.45.Gd, 82.65.Dp, 64.70.Fx, 68.35.Md

I. Introduction

Unless much experimental care is provided in growing crystals and cutting them, generally on an atomic scale their surfaces exhibit an irregular topography. Numerous theoretical [1-10] and experimental [11-14] studies have demonstrated that if such real surfaces are exposed to a vapor phase the resulting wetting phenomena [15,16] may differ significantly from the corresponding ones on perfectly planar surfaces of the same substrate-fluid systems. These studies are focused on the properties of the adsorbed liquid films averaged laterally over the statistical irregularities of the substrate topography.

However, e.g., in the context of structured semiconductor surfaces [17-19], microfluidics [20-24], and templates for the selfassembly of small particles [25-27] highly *regular* nonflat lateral surface structures can be produced. But both the theoretical understanding of the *local* wetting phenomena in such structures [28-42] as well as corresponding experimental investigations [43,44] are still in their infancies [45].

As a paradigm of such structures we consider a single wedgelike cavity with an opening angle 2φ and macroscopic extension along its edge; along this y direction the system is taken to be translationally invariant (see Fig.1(a)). The wedge is filled with a simple, volatile fluid such that the bulk, i.e., far away from the edge at $x = z = 0$, is occupied by the vapor phase with temperature T and chemical potential μ . The values of μ are chosen such that the bulk is close to liquid-vapor coexistence $\mu_0(T)$. (Our considerations are equally applicable to the two fluid phases of a phase separated binary liquid mixture.) Accordingly, under the influence of the substrate potential a liquidlike wetting film will form at the planar surfaces leading to a meniscus near the edge. We analyze the height of this meniscus and its shape as a function of μ and T . This analysis is based on thermodynamic considerations (Sec.II) and on a phenomenological interface model for the local height of the meniscus (Sec.III). For a special choice of the effective interfacial potential we are able to calculate analytically the shape of the interface in the wedge explicitly (Sec.IV). By considering a suitably chosen Landau-Ginzburg-Wilson theory for an order parameter in this geometry (Sec.V) we can discuss the range of validity for the effective interface model studied in Sec.III. Our results

are summarized in Sec.VI.

II. Macroscopic description

In Secs.III and IV we shall analyze microscopically the formation of a meniscus of a *volatile* liquid in thermal equilibrium with its vapor phase. Nonetheless it will turn out to be instructive to consider first in the following subsections the corresponding macroscopic description of the problem in constrained equilibrium and to refer to the results obtained within the standard theory of capillarity.

A. Constrained equilibrium and thermodynamics

We consider a symmetric wedge (i.e., both walls consist of the same type of substrate material) with opening angle $2\varphi < \pi$ (see Fig.1(a)). It is cut off at a macroscopic height H_0 . The lower part of the wedge is filled with liquid; the corresponding wall-liquid, vapor-liquid, and wall-vapor surface tensions are denoted as σ_{wl} , σ_{lg} , and σ_{wg} , respectively. The vapor and liquid phases are taken to be at bulk equilibrium so that they can exchange volume with no cost in *bulk* free-energy. However, in this subsection we consider a constrained equilibrium such that the volume V of the liquid phase is prescribed. The liquid meniscus is enclosed by the walls at $z = |x| \cot \varphi$ and the liquid-vapor interface is described by $f(x)$ (see Fig.1(a)). Here and in the following we discuss a two-dimensional wedge. Some aspects of the full three-dimensional case will be discussed in Subsec.IIB. In the present macroscopic description all length scales are much larger than atomic scales so that the free energy F of the system is determined by the aforementioned *surface* tensions only. For a given configuration of the interface $f(x)$ one has (see Fig.1(a))

$$F[f] = \sigma_{lg} \int_{-x_1}^{x_1} dx \sqrt{1 + f_x^2(x)} + 2 \frac{x_0 - x_1}{\sin \varphi} \sigma_{wg} + 2 \frac{x_1}{\sin \varphi} \sigma_{wl} \quad (2.1)$$

with $f_x = \frac{df}{dx}$. In Eq.(2.1) the artificial contributions to the free energy generated by the cutoff at $z = H_0$ have been omitted. The liquid-gas interface intersects the walls at $x = \pm x_1$

with $f(\pm x_1) = x_1 \cot \varphi$. The surface tensions determine the contact angle Θ via the Young equation

$$\cos \Theta = \frac{\sigma_{wg} - \sigma_{wl}}{\sigma_{lg}} . \quad (2.2)$$

The difference $\Delta F[f] = F[f] - 2 x_0 \sigma_{wg}/\sin \varphi$ of the energies of the wedge with a given amount of liquid and of the wedge filled by the gas phase only follows from Eq.(2.1) by subtracting the term $2 x_0 \sigma_{wg}/\sin \varphi$. Accordingly the constrained equilibrium profile \bar{f} minimizes the functional

$$\Delta F^*[f] = \sigma_{lg} \int_{-x_1}^{x_1} dx \left\{ \sqrt{1 + f_x^2(x)} - \frac{\cos \Theta}{\sin \varphi} + \frac{\lambda}{\sigma_{lg}} (f(x) - |x| \cot \varphi) \right\} \quad (2.3)$$

with the boundary conditions $f(\pm x_1) = x_1 \cot \varphi$ and where the Lagrange multiplier λ implements the constraint of constant liquid volume

$$V = \int_{-x_1}^{x_1} dx (f(x) - |x| \cot \varphi) . \quad (2.4)$$

(In these formulae $f(x)$ is regarded as a single-valued function. In the case that $f(x)$ consists of two branches the corresponding separate analysis for each of the two branches leads to the same conclusions as the ones described below. Moreover it is necessary to assume that $\Theta + \varphi < \pi$; otherwise neither the interface nor its branches can be regarded as single valued functions.) According to the standard calculus of variations [46] the equilibrium profile fulfills the differential equation

$$\frac{\bar{f}_{xx}}{(1 + \bar{f}_x^2)^{\frac{3}{2}}} = \frac{\lambda}{\sigma_{lg}} \quad (2.5)$$

with the boundary conditions

$$\frac{1 \pm \bar{f}_x(\pm x_1) \cot \varphi}{(1 + \bar{f}_x^2(\pm x_1))^{\frac{1}{2}}} = \frac{\cos \Theta}{\sin \varphi} . \quad (2.6)$$

Equation (2.6) is equivalent to the statement that the angle between the liquid-gas interface and the wall (measured on the liquid side of the interface) is equal to the contact angle Θ

in the planar case. Thus the equilibrium profile is given by a part of a circle whose radius $R = \frac{\sigma_{lg}}{\lambda}$ follows from the constant volume constraint (Eq.(2.4)) and intersects the walls at the contact angle Θ . For $\Theta < \frac{1}{2}\pi - \varphi$, the liquid-gas interface is concave, while for $\Theta > \frac{1}{2}\pi - \varphi$ the interface is convex; $\Theta = \frac{1}{2}\pi - \varphi$ corresponds to a flat interface. The center of the circle is located at (x_c, z_c) with

$$x_c = 0, \quad z_c = -R \operatorname{sign} \left(\Theta + \varphi - \frac{1}{2}\pi \right) \frac{\cos \Theta}{\sin \varphi}, \quad (2.7)$$

where the radius R is given by

$$R = \sqrt{V} \left(\Theta + \varphi - \frac{1}{2}\pi + \frac{\cos \Theta \cos(\Theta + \varphi)}{\sin \varphi} \right)^{-\frac{1}{2}}. \quad (2.8)$$

The value of z_c is always positive for a concave interface while for the convex one it can be either positive or negative, depending on the value of the contact angle Θ . The intersection of the circle with the wall occurs at

$$x_1 = -R \operatorname{sign} \left(\Theta + \varphi - \frac{1}{2}\pi \right) \cos(\Theta + \varphi). \quad (2.9)$$

In the case that the liquid forms a bridge connecting the walls the free energy is given by

$$\begin{aligned} F[f_1, f_2] = \sigma_{lg} \int_{-x_1}^{x_1} dx \sqrt{1 + f_{1x}^2(x)} + \sigma_{lg} \int_{-x_2}^{x_2} dx \sqrt{1 + f_{2x}^2(x)} + \\ + 2 \frac{x_0 - x_1 + x_2}{\sin \varphi} \sigma_{wg} + 2 \frac{x_1 - x_2}{\sin \varphi} \sigma_{wl} \end{aligned} \quad (2.10)$$

where $f_1(x)$ and $f_2(x)$ correspond to the upper and lower liquid-gas interface, respectively, while $\pm x_1$ and $\pm x_2$ denote the intersections with the walls. The minimization of the constrained free energy with respect to f_1 and f_2 leads to the conclusion that both interfaces are parts of the same circle whose center is given by Eq.(2.7). For each of them the corresponding contact angle (measured on the liquid side of the interface) has the same value Θ as given by the contact angle for a planar substrate.

The bridge can exist if and only if z_c is positive and larger than the radius of the circle, i.e., if $\Theta > \frac{1}{2}\pi + \varphi$. In this case the radius of the bridge has the value

$$R = \sqrt{V} (2\Theta - \pi - \sin 2\Theta)^{-\frac{1}{2}} . \quad (2.11)$$

Thus, depending on the opening angle φ and the contact angle Θ , the possible shapes of a liquid meniscus can be summarized as follows (see Fig.2):

$$\begin{aligned} \Theta > \frac{1}{2}\pi + \varphi &: \text{bridge} \\ \frac{1}{2}\pi + \varphi \geq \Theta > \frac{1}{2}\pi - \varphi &: \text{single convex interface} \\ \Theta = \frac{1}{2}\pi - \varphi &: \text{flat interface} \\ \frac{1}{2}\pi - \varphi > \Theta &: \text{concave interface} . \end{aligned}$$

For these configurations the difference in free energy between the wedge being filled with a liquid of volume V and vapor otherwise and the wedge being filled with vapor only is given by

$$\Delta F = \text{sign} \left(\Theta + \varphi - \frac{\pi}{2} \right) 2\sigma_{lg} \sqrt{V} \left(\Theta + \varphi - \frac{\pi}{2} + \frac{\cos \Theta \cos(\Theta + \varphi)}{\sin \varphi} \right)^{\frac{1}{2}} , \quad (2.12)$$

single interface ,

and

$$\Delta F = 4\sigma_{lg} \sqrt{V} \left(2\varphi + \cos^2 \Theta \cot \varphi \right) (2\Theta - \pi - \sin 2\Theta)^{-\frac{1}{2}} , \text{ bridge.} \quad (2.13)$$

Any configuration with more than one bridge is disfavored by a higher free energy. $\Theta = \frac{1}{2}\pi + \varphi$ corresponds to the border case between a bridge and a convex interface for which the lowest point of the bridge coincides with the corner of the wedge.

From Eq.(2.12) one can infer that for $\Theta > \frac{1}{2}\pi - \varphi$, i.e., for a single convex interface or a bridge, ΔF decreases upon decreasing the liquid volume down to the limiting value $V = 0$. On the other hand, for $\Theta < \frac{1}{2}\pi - \varphi$ the free energy decreases upon increasing V , i.e., upon filling the whole wedge with liquid. Therefore

$$\Theta = \frac{1}{2}\pi - \varphi \quad (\text{wetting}) \quad (2.14)$$

marks a filling transition for the wedge. This case corresponds to a flat interface (see Fig.2) and the corresponding free energy is independent of the volume of the liquid. At

fixed temperature, i.e., Θ fixed, a wide wedge is covered only by a microscopically thin liquid film which turns into a macroscopic meniscus upon narrowing the wedge beyond the critical opening angle $\varphi_c = \frac{1}{2}\pi - \Theta$. (These considerations can be extended to the case of a nonsymmetric wedge. The corresponding results are presented in Appendix A.) If the planar walls undergo a wetting transition the contact angle $\Theta(T)$ decreases as a function of temperature and vanishes at $T = T_w$, i.e., $\Theta(T = T_w) = 0$.

Thus for a fixed opening angle Eq.(2.14) defines implicitly a filling transition temperature T_φ such that $\Theta(T_\varphi) = \frac{1}{2}\pi - \varphi$. One has $T_\varphi < T_w$ and $T_{\varphi \rightarrow \frac{1}{2}\pi} = T_w$. This means that the wedge undergoes a filling transition at a temperature at which the outer parts of the wedge far away from the center still remain nonwet. The same conclusion has been reached previously by Hauge from phenomenological considerations based on the Laplace and Young equations [34]. Here we obtain this conclusion by analyzing the free energy of the system.

However, as long as the volume of the liquid drop has a fixed value there is no phase transition and the free energy is an analytical function of temperature and of the wedge opening angle. Close to $\varphi = \frac{1}{2}\pi - \Theta$ it can be expanded into a series of powers of $(\varphi - (\frac{1}{2}\pi - \Theta))$. The dominant term of this expansion is

$$\Delta F = \simeq -2\sigma_{lg} \sqrt{V \cot \varphi} \left(\varphi - \left(\frac{1}{2}\pi - \Theta \right) \right) . \quad (2.15)$$

The aforementioned qualitative change of the interfacial shape and the change of the behavior of the free energy upon increasing V are traces of the filling transition which comes into play when the fixed-volume constraint is removed and the system is at liquid-gas bulk coexistence of a grand canonical ensemble. The minimization of the functional $\Delta F[f]$ instead of the functional $\Delta F^*[f]$ leads to the following equation for the equilibrium interfacial shape:

$$\frac{\bar{f}_{xx}}{(1 + \bar{f}_x^2)^{\frac{3}{2}}} = 0 . \quad (2.16)$$

Thus the interface is flat and horizontal. (In the general case of a nonsymmetric wedge the interface still remains flat but not necessarily horizontal.) In the case of a nonconstrained system the surface free-energy is given by

$$F(H) = \frac{2}{\cos \varphi} [H_0 \sigma_{wg}(T) + H(\cos \Theta(T_\varphi) - \cos \Theta(T)) \sigma_{lg}(T)] , \quad (2.17)$$

where H is the height of the flat and horizontal interface measured from the edge of the wedge. For $T < T_\varphi$ the above surface contribution is minimized by $H = 0$, while for $T > T_\varphi$ this contribution is minimized by the largest possible value for H . The latter case corresponds to a wedge completely filled by the liquid. The relevant surface free energy has the following form:

$$F = \frac{2 H_0}{\cos \varphi} \begin{cases} \sigma_{wg}(T) & , T \leq T_\varphi, \\ \sigma_{wg}(T) + (\cos \Theta(T_\varphi) - \cos \Theta(T)) \sigma_{lg}(T) & , T \geq T_\varphi, . \end{cases} \quad (2.18)$$

According to Eq.(2.18) F is continuous at $T = T_\varphi$ but exhibits a break in slope as function of temperature. Thus the filling transition in a wedge is – similar to a wetting transition on a planar substrate – associated with a singularity in the corresponding *surface* contribution to the free energy. But the relevant structural properties such as, e.g., the shape of the microscopically thin liquid film covering the wedge are determined by the *line* contribution to the free energy which is singular at T_φ , too. This differs from the wetting transition for which all relevant structural properties are determined by the surface free energy alone.

An analogous analysis excludes a bridge as a stable configuration for the unconstrained system. Again both interfaces for such a bridge must be flat. If their heights are denoted as H_1 and $H_2 < H_1$, respectively, the free energy is given by

$$F(H_1, H_2) = \frac{2}{\cos \varphi} [H_0 \sigma_{wg}(T) + H_1 (\cos \Theta(T_\varphi) - \cos \Theta(T)) \sigma_{lg}(T) + H_2 (\cos \Theta(T_\varphi) + \cos \Theta(T)) \sigma_{lg}(T)] . \quad (2.19)$$

Below T_φ this expression is minimized by $H_1 = 0$ and $H_2 = 0$. Above T_φ the minimum corresponds to $H_2 = 0$ while H_1 takes its maximal possible value.

In the above considerations we have discussed a wetting situation, i.e., the bulk is occupied by vapor and the wedgelike substrate prefers the liquid. Our results can be easily mapped onto the corresponding drying situation in which the bulk is occupied by liquid and

the wedgelike substrate prefers the vapor phase. In this case the filling transition of the wedge occurs for

$$\Theta = \frac{1}{2}\pi + \varphi \text{ (drying).} \quad (2.20)$$

This is in accordance with Eq.(2.14) because liquid and gas are interchanged but the contact angle is in both cases taken to be the one of the liquid phase, i.e., in Eq.(2.14) Θ must be replaced by $\pi - \Theta$. If the planar substrate supports the drying transition, i.e., $\Theta(T \rightarrow T_d) = \pi$, the wedge will be completely filled by the vapor phase for $T > T_\varphi$ where now $\Theta(T = T_\varphi) = \frac{1}{2}\pi + \varphi$. Again one has $T_\varphi < T_d$ and $T_{\varphi \rightarrow \frac{1}{2}\pi} = T_d$. Equation (2.20) states that, under drying conditions, for all temperatures corresponding to $\Theta(T) < \frac{1}{2}\pi$ there is no opening angle φ_c such that the wedge is filled with vapor for $\varphi < \varphi_c$. On the other hand, if $\Theta(T) > \frac{1}{2}\pi$ there is always a sufficiently small opening angle $\varphi_c(T) = \Theta(T) - \frac{1}{2}\pi$ such that the wedge is filled up with vapor for $\varphi < \varphi_c$.

This observation may be of relevance for preparing super water-repellent surfaces [47]. These are surfaces which exhibit a contact angle $\pi > \Theta > \frac{1}{2}\pi$ if they are very smooth. On the other hand, if the surfaces – made of the same material – are prepared such that they exhibit a very porous structure one observes an apparent contact angle close to π [47]. In the present context this observation is in accordance with a filling of (wedge-like) pores with vapor at temperatures at which the smooth planar surface is not yet dry, i.e., $\Theta < \pi$.

Similar considerations hold for wetting conditions, i.e., when the wedge is exposed to a vapor phase. Equation (2.14) states that for all temperatures corresponding to $\Theta(T) > \frac{1}{2}\pi$ there is no opening angle φ_c such that the wedge is filled with liquid for $\varphi < \varphi_c$. On the other hand, if $\Theta(T) < \frac{1}{2}\pi$ there is always a sufficiently small opening angle $\varphi_c(T) = \frac{1}{2}\pi - \Theta(T)$ such that the wedge is filled with liquid for $\varphi < \varphi_c$.

B. Theory of capillarity

In the previous two subsections we have considered the constrained equilibrium of fluid configurations which are translationally invariant along the y direction of the edge of the

wedge. Effectively this corresponds to a two-dimensional system. In a three-dimensional system, a fixed finite volume V of the liquid must have a finite extension in the y direction and thus the shape $f(x, y)$ of the liquid-vapor interface depends also on y . Based on the classical Young-Laplace-Gauss capillarity theory the equilibrium liquid-vapor interface configurations are surfaces of constant mean curvature meeting the bounding walls with contact angle Θ .

There exists a sizable body of literature devoted to the solution of this problem for the present wedge geometry (see, e.g., Refs.[48-53] and references therein). The most recent account of the present knowledge based on mathematically rigorous results and numerical evidence is summarized in Fig.6 in Ref.[53].

For $\Theta > \frac{1}{2}\pi$ there are two possible liquid configurations depending on the opening angle 2φ . For $\varphi \geq \Theta - \frac{1}{2}\pi > 0$ an edge blob forms; this is a part of a sphere such that the liquid is in contact with both walls and the edge of the wedge. The shape of the liquid-vapor interface is convex. If the opening angle of the wedge is reduced such that $\varphi < \Theta - \frac{1}{2}\pi > 0$ the liquid loses contact with the edge of the wedge and a spherical bridge connecting the two walls is formed. The transition between these two distinct configurations occurs at $\varphi = \Theta - \frac{1}{2}\pi > 0$. This means that a preference of the planar substrate for the vapor phase, i.e., $\Theta > \frac{1}{2}\pi$ implies a prefilling of the wedge with vapor for sufficiently small opening angles of the wedge.

For $\Theta < \frac{1}{2}\pi$ a tubular bridge between the walls is not possible. For a wide wedge with $\varphi > \frac{1}{2}\pi - \Theta > 0$ one finds an edge blob in contact with both walls and with the edge of the wedge. Upon decreasing the opening angle of the wedge at $\varphi = \frac{1}{2}\pi - \Theta > 0$ a transition to edge spreading occurs which persists for $\varphi \leq \frac{1}{2}\pi - \Theta > 0$. Edge spreading by the liquid is not possible for $\Theta > \frac{1}{2}\pi$. This means that a preference of the planar substrate for the vapor phase, i.e., $\Theta > \frac{1}{2}\pi$ implies a prefilling of the wedge with vapor for sufficiently small opening angles of the wedge. These findings are in full accordance with the free energy analysis of the effectively two-dimensional system discussed in Subsec.IIA.

III. Description of filling transitions by an interface model

Within the macroscopic description in Sec.II the type of substrate forming the wedge enters only summarily via the surface tensions σ_{wg} and σ_{wl} . In the actual microscopic picture the fluid particles are exposed to the external substrate potential $V(x, z)$ exerted by the particles forming the wedge. The resulting full number density distribution $\rho(x, z)$ of the fluid particles can be determined, e.g., either by simulations or by density functional theory. However, in view of the considerable numerical challenges by such an approach so far only hard sphere fluids confined by hard walls have been studied in such full detail [40,41]. The accessible system sizes of the wedges which can be studied within these approaches are also severely limited. Moreover, without attractive interactions the hard-body systems do not exhibit filling transitions.

A. Effective interface Hamiltonian

The study of effective models for the liquid-vapor interface exposed to an effective interface potential [54,55], which takes into account the competition between the substrate potential and the interaction potential between the fluid particles, serves as a reasonable compromise between a full-fledged microscopic theory and the purely macroscopic picture. Within this effective approach the morphology of the liquid-vapor interface is determined by the effective interface Hamiltonian (see Fig.1(b))

$$\mathcal{H}[l] = \int_{-\infty}^{\infty} dx \left\{ \sigma_{lg} \left(\sqrt{1 + \left(\frac{df(x)}{dx} \right)^2} - \sqrt{1 + \cot^2 \varphi} \right) + \frac{V(l(x) \sin \varphi) - V(l_\infty \sin \varphi)}{\sin \varphi} \right\}. \quad (3.1)$$

Since $z = |x| \cot \varphi$ is the position of the surfaces of the wedge, the local thickness of the liquid film measured vertically equals $l(x) = f(x) - |x| \cot \varphi$ and thus exhibits a cusp at $x = 0$ with $l'(x \rightarrow \pm 0) = \mp \cot \varphi$. Thus the first term in Eq.(3.1) corresponds to the cost in free energy due to the increase of the surface area of the liquid-vapor interface relative to its flat configuration at $|x| = \infty$ where $\left| \frac{df}{dx}(x \rightarrow \infty) \right| = \cot \varphi$ so that $\sqrt{1 + \cot^2(\varphi)} = \frac{1}{\sin \varphi}$. The second part of the Hamiltonian takes into account the effective interaction V between the liquid-vapor interface and the wedge-shaped substrate relative to the configuration $l(|x| \rightarrow$

$\infty) = l_\infty$. V denotes the effective interface potential which we take to be of the same form as for a horizontal liquid-vapor interface interacting with the corresponding planar substrate [54,55]:

$$V(L) = \sigma_{wl} + \sigma_{lg} + \omega(L) + \Delta\mu \Delta\rho L \quad (3.2)$$

with $\omega(L \rightarrow \infty) = 0$, $\Delta\mu = \mu_0(T) - \mu$, and $\Delta\rho = \rho_l - \rho_g$ where ρ_l and ρ_g are the number density of the liquid and vapor, respectively. In Eq.(3.1) $V(L)$ is evaluated in a local approximation such that $L = l(x) \sin \varphi$ is the local thickness of the wetting film normal to the *near* surface of the substrate; therefore these potential terms are integrated with respect to $\frac{dx}{\sin \varphi}$, i.e., along the substrate surface (see Fig.1(b)). Thus Eq.(3.1) neglects the additional effective interaction of the liquid-vapor interface with the *distant* substrate surface. This approximation is expected to be valid for a rather open wedge (see below). The equilibrium film thickness on a planar substrate minimizes $V(L)$ and yields the actual substrate-vapor surface tension $\sigma_{wg} = V(l_\infty \sin \varphi)$ of the planar substrate. Due to the subtraction of those terms which correspond to the asymptotic behavior for $x \rightarrow \pm\infty$ the Hamiltonian $\mathcal{H}[l]$ is finite for all configurations compatible with the boundary conditions. Therefore $\mathcal{H}[l]$ describes the *line contribution* to the free energy associated with the linear extension L_y of the wedge in the y direction. In the present mean-field theory we neglect the fluctuations of the interface along the y direction so that f depends on x only and the line contribution carries simply a factor L_y which has been omitted in Eq.(3.1). We emphasize that this consideration of the line contribution to the free energy represents the most important improvement over the macroscopic description which considers only surface contributions. Within mean-field theory the equilibrium shape $\bar{f}(x)$ of the meniscus minimizes this line contribution:

$$\sigma_{lg} \frac{\frac{d^2 \bar{f}(x)}{dx^2}}{\left(1 + \left(\frac{d\bar{f}(x)}{dx}\right)^2\right)^{\frac{3}{2}}} = V'((\bar{f}(x) - |x| \cot \varphi) \sin \varphi) , \quad (3.3)$$

$$\bar{f}'(0) = 0 , \quad \bar{f}(x \rightarrow \pm\infty) = l_\infty + |x| \cot \varphi .$$

Equation (3.3) is known as the so-called augmented Young equation and has been studied by Kagan et al. [39] but not with the view of filling phase transitions; recently these authors extended their analysis to study eye-shaped capillaries [56]. Due to the symmetry of the system we confine our subsequent analysis to $x \geq 0$. In terms of $l(x)$ the boundary conditions are $l(x \rightarrow \infty) = l_\infty \sin \varphi$ and $l'(x = 0+) = -\cot \varphi$. Integrating Eq.(3.3) yields

$$\sigma_{lg} \left(1 - \frac{\sin \varphi + \cos \varphi \frac{d\bar{f}(x)}{dx}}{\sqrt{1 + \left(\frac{d\bar{f}}{dx} \right)^2}} \right) = V(\bar{l}(x) \sin \varphi) - V(l_\infty \sin \varphi) . \quad (3.4)$$

With $\bar{f}'(0) = 0$ and $l_0 \equiv \bar{l}(x = 0)$ one obtains from Eq.(3.4)

$$\frac{\Delta V}{\sigma_{lg}} \equiv \frac{1}{\sigma_{lg}} [V(l_0 \sin \varphi) - V(l_\infty \sin \varphi)] = 1 - \sin \varphi \equiv \bar{v}(\varphi) . \quad (3.5)$$

Equation (3.5) is an implicit algebraic equation for the filling height l_0 in the center of the wedge in terms of the opening angle φ and the wetting properties of the planar system, i.e., σ_{lg} , $V(L)$, and thus l_∞ . At liquid-vapor coexistence $V(L \rightarrow \infty) = \sigma_{wl} + \sigma_{lg}$ (Eq.(3.2)) with $\frac{\Delta V}{\sigma_{lg}}(L \rightarrow \infty) = 1 - \cos \Theta$ (Eq.(2.2)) so that the condition for the filling transition $\bar{l}(0) \rightarrow \infty$ can be expressed in terms of the contact angle Θ of the planar system (Eq.(2.2)):

$$\cos \Theta(T_\varphi) = \sin \varphi \quad \text{or} \quad \Theta(T_\varphi) = \frac{1}{2}\pi - \varphi . \quad (3.6)$$

T_φ is the lowest temperature for which $l_0 = \infty$. Thus our microscopic approach confirms the results for T_φ as predicted by the macroscopic theory in Sec.II. (This conclusion even holds if the integrand in Eq.(3.1) is supplemented by a term proportional to the mean curvature of the interface.) It is rather satisfactory to see *explicitly* that a microscopic theory for the line contribution to the free energy renders the same value for the filling transition temperature T_φ as the macroscopic considerations based on the surface free energies. On the other hand this is to be expected because at T_φ the surface free energy of the wedge is nonanalytic (see Eq.(2.18)) so that the line free energy has to follow suit. This is analogous to the fact that surface free energies are nonanalytic at bulk transitions.

Before we turn to a closer analysis of the filling transition we note that in the special case of a wide open wedge, i.e., $\varphi = \frac{1}{2}\pi - \epsilon$ with $\epsilon \ll 1$ the effective interface Hamiltonian in Eq.(3.1) reduces to (see Appendix B)

$$\mathcal{H}[f] = \int_{-\infty}^{\infty} dx \left\{ \frac{\sigma_{lg}}{2} \sin \varphi \left[\left(\frac{df(x)}{dx} \right)^2 - \cot^2 \varphi \right] + \frac{V(l(x) \sin \varphi) - V(l_\infty \sin \varphi)}{\sin \varphi} \right\}, \quad \left| \frac{1}{2}\pi - \varphi \right| \ll 1, \quad (3.7)$$

so that the equilibrium profile $\bar{f}(x) = \bar{l}(x) + |x| \cot \varphi$ is determined by

$$\sigma_{lg} \sin \varphi \frac{d^2 \bar{l}(x)}{dx^2} = V'(\bar{l}(x) \sin \varphi), \quad x > 0. \quad (3.8)$$

Upon integration one obtains with $\frac{d\bar{l}}{dx}(x = +\infty) = 0$

$$\frac{1}{2} \sigma_{lg} \sin^2 \varphi \left(\frac{d\bar{l}(x)}{dx} \right)^2 = V(\bar{l}(x) \sin \varphi) - V(l_\infty \sin \varphi). \quad (3.9)$$

Thus for the filling height l_0 in the center of the wedge one finds due to $\frac{d\bar{l}}{dx}(x \rightarrow \pm 0) = \mp \cot \varphi$ (compare Eq.(3.5)

$$\frac{\Delta V}{\sigma_{lg}} = \frac{1}{2} \cos^2 \varphi \equiv v(\varphi). \quad (3.10)$$

According to the relations $\frac{1}{2} \cos^2 \varphi = (1 - \sin \varphi) \cos^2(\frac{1}{2}(\frac{1}{2}\pi - \varphi))$ and $1 - \sin \varphi = 2 \sin^2(\frac{1}{2}(\frac{1}{2}\pi - \varphi))$ the approximate implicit equation (3.10) for l_0 differs from the corresponding full equation (3.5) only by terms of the order ϵ^4 : $v(\varphi) = \bar{v}(\varphi)(1 + O(\epsilon^2))$ and $\bar{v}(\varphi) = O(\epsilon^2)$. This is also true for the equation for the filling transition temperature T_φ (compare Eq.(3.6))

$$\begin{aligned} \cos \Theta(T_\varphi) &= 1 - \frac{1}{2} \cos^2 \varphi, \quad \left| \frac{1}{2}\pi - \varphi \right| \ll 1, \\ &= \sin \varphi + 2 \sin^4 \left(\frac{1}{2} \left(\frac{1}{2}\pi - \varphi \right) \right). \end{aligned} \quad (3.11)$$

Thus we conclude that Eqs.(3.7)-(3.11) are reliable approximations for a wide open wedge.

B. Filling height

In the implicit equation (3.5) and its approximation (Eq.(3.10)) the right hand side $\bar{v}(\varphi)$ and $v(\varphi)$, respectively, do not depend on l_0 ; furthermore the left hand side $\Delta V/\sigma_{lg}$ remains unchanged upon the open wedge approximation. This facilitates a transparent graphical solution for the filling height l_0 as shown in Figs.3 and 4. As anticipated the filling height l_0 is larger than the wetting film thickness l_∞ on the walls of the wedge far away from the edge of the wedge. At gas-liquid coexistence, i.e., $\Delta\mu = 0$ the filling height l_0 diverges smoothly for $T \nearrow T_\varphi$ in the case of critical wetting and jumps to a macroscopic value in the case of first-order wetting of the corresponding planar substrate. At $T = T_\varphi$ the wetting film thickness l_∞ asymptotically far away from the center of the wedge remains finite. Thus within the present model we find that the wedge does indeed undergo a filling transition at T_φ and that the order of the filling transition agrees with the order of the wetting which takes place at $T_w > T_\varphi$ on the corresponding planar substrate for which $\Theta(T \rightarrow T_w) = 0$.

As will be discussed in more detail in the following subsection the filling height l_0 diverges along isotherms $\Delta\mu \rightarrow 0$ for $T > T_\varphi$. In that case in Eq.(3.5) the asymptotic behavior of $V(L \rightarrow \infty) = \Delta\mu\Delta\rho L + \sigma_{wl} + \sigma_{lg}$ can be used. Together with $V(l_\infty \sin \varphi) = \sigma_{wg}$ and Eq.(2.2) this leads to $\Delta V/\sigma_{lg} \rightarrow \Delta\mu\Delta\rho l_0 \sin \varphi/\sigma_{lg} + 1 - \cos \Theta$ so that from Eq.(3.5) one obtains

$$l_0(\Delta\mu \rightarrow 0, T > T_\varphi) = \frac{\cos \Theta - \sin \varphi}{\sin \varphi} \frac{\sigma_{lg}}{\Delta\rho} \frac{1}{\Delta\mu} . \quad (3.12)$$

We note that the form of Eq.(3.12) is valid irrespective of the order of the filling transition and irrespective of the range of the molecular forces. The latter enter only indirectly via Θ , σ_{lg} , and $\Delta\rho$. Equation (3.12) is in full agreement with the macroscopic description in Ref.[34] and the numerical results above T_w in Ref.[33].

C. Line tension

As apparent from Figs.3 and 4 the implicit equation (Eqs.(3.5) and (3.10)) for the filling height l_0 yields two or even more solutions. For $l_0 < \infty$, i.e., for $T < T_\varphi$ with T_φ defined by Eqs.(2.14) and (3.6) or for $\Delta\mu > 0$, the equilibrium solution is that one whose corresponding

profile $l(x)$ with $l(0) = l_0$ minimizes the line contribution of the free energy (Eqs.(3.1) or (3.7)). For $l_0 < \infty$ all competing configurations have the same surface free energy. At coexistence, i.e., for $\Delta\mu = 0$, l_0 can become macroscopically large. In that case one has to consider both the line and the surface contribution such that if one solution has a lower surface energy it wins out irrespective of the behavior of the line tension; the line tensions matter only if the surface free energies are equal. (By construction the bulk free energies of all configurations are always the same.) Nonetheless, in any case it is interesting to study the thermodynamic behavior of line tension.

From Eq.(2.18) one infers that at coexistence the temperature dependence of the surface free energy density is given by $\sigma_{wg} + \delta\sigma(T)$ with $\delta\sigma(T < T_\varphi) = 0$ and $\delta\sigma(T > T_\varphi) < 0$ due to $\sigma_{lg}(T) > 0$. This implies that for $T > T_\varphi$ the filled wedge exhibits a surface free energy which is lower than the surface free energy of the unfilled wedge extrapolated to $T > T_\varphi$. This holds independently of whether $\sigma_{wg}(T)$ is an increasing or decreasing function of T . Thus we conclude that $l_0 = \infty$ for all thermodynamic states ($\Delta\mu = 0, T > T_\varphi$).

For all other thermodynamic states with $\Delta\mu \geq 0$ one has $l_0 < \infty$ and the line contribution to free energy (Eq.(3.7)) of the corresponding profile $f(x)$ can be determined explicitly. From Eq.(3.9) one has $\frac{dl}{dx} = \mp(\sqrt{2}/(\sqrt{\sigma_{lg}} \sin \varphi))\sqrt{V(l(x) \sin \varphi) - V(l_\infty \sin \varphi)}$ for $x > 0$ (upper sign) or $x < 0$ (lower sign). With $\frac{df}{dx} = \frac{dl}{dx} \pm \cot \varphi$ for $x > 0$ (upper sign) or $x < 0$ (lower sign) the insertion into Eq.(3.7) yields for the line tension η

$$\eta = 2\sqrt{2}\sigma_{lg} A \quad (3.13)$$

with

$$A = \int_{l_\infty}^{l_0} dl \left\{ \sqrt{\frac{V(l \sin \varphi) - V(l_\infty \sin \varphi)}{\sigma_{lg}}} - \sqrt{\frac{V(l_0 \sin \varphi) - V(l_\infty \sin \varphi)}{\sigma_{lg}}} \right\} \quad (3.14)$$

where l_0 is a solution of Eq.(3.10) and l_∞ minimizes $V(L)$. The quantity A , which has the dimension of a length and which gives the line tension up to the positive prefactor $2\sqrt{2}\sigma_{lg}$, is the area between the curves $\sqrt{(V(l \sin \varphi) - V(l_\infty \sin \varphi))/\sigma_{lg}}$, $\sqrt{v(\varphi)} = \sqrt{(V(l_0 \sin \varphi) - V(l_\infty \sin \varphi))/\sigma_{lg}}$ (see Eq.(3.10)), and $l = l_\infty$ (see Figs.5 and 6). Note that

obviously the curves ΔV and $v(\varphi)$ intersect at the same position l_0 as $\sqrt{\Delta V}$ and $\sqrt{v(\varphi)}$. From this graphical interpretation one infers immediately that only the solutions $l_0 > l_\infty$ have to be taken into account; as expected the filling height in the center of the wedge is larger than the thickness of the wetting film far outside and these solutions are the ones which increase for $T \nearrow T_\varphi$.

One can infer the filled state for $\Delta\mu = 0$ and $T > T_\varphi$ by considering isotherms $\Delta\mu \rightarrow 0$ for $T > T_\varphi$ (see Eq.(3.12)). Figure 7(a) describes the continuous filling of the wedge for $T > T_\varphi$ and $\Delta\mu \rightarrow 0$ in the case of a critical wetting transition. For an underlying first-order wetting transition Fig.7(b) demonstrates that, along an isotherm with $T > T_\varphi$, at $\Delta\mu_{pf}(T)$ one encounters a thin-thick transition of the filling height which is *not* accompanied by a phase transition in the structure of the wetting film far away from the center of the wedge. We call this phase transition a *prefilling transition*. Once this prefilling transition locus has been passed, the filling height l_0 diverges continuously for $\Delta\mu \rightarrow 0$ (see Eq.(3.12)). This confirms, within the present interface model, the expectation that the thermodynamic states $(\Delta\mu = 0, T > T_\varphi)$ correspond to a filled wedge. The order of the filling transition at coexistence is linked to the order of the underlying wetting transition.

From Fig.7(b) one infers that a jump in the thickness l_∞ of the wetting film far away from the center of the wedge upon crossing the prewetting line enforces a discontinuity in the line contribution to free energy associated with a discontinuity of the whole profile $l(x)$, however such, that – surprisingly – $l_0 = l(x = 0)$ happens to change only smoothly. On the other hand, upon crossing the prefilling line l_0 changes discontinuously without a change in l_∞ . This behavior confirms the general picture that a nonanalyticity at one thermodynamic level (bulk, surface, line, ...) induces nonanalyticities at the same locus at all subdominant thermodynamic levels and that each thermodynamic level can develop new nonanalyticities at loci where all higher thermodynamic levels are strictly analytic: the phase boundaries in the bulk free energy are lines of nonanalyticities both for the surface and the line contributions, and the prewetting line nonanalyticity of the surface free energy

is also the locus of nonanalyticities in the line tension. On the other hand the bulk free energy is analytic along the prewetting line and the bulk and the surface free energy are analytic along the prefilling line.

If the wedge fills, on each side of the wedge a three-phase contact line between the substrate, liquid, and vapor is forming. In the limit $l_0 \rightarrow \infty$ these two contact lines become independent and each of them reduces to the structure of a single three-phase contact line on a planar substrate. Therefore one expects that in the limit $l_0 \rightarrow \infty$ the line tension given by Eqs.(3.13) and (3.14) should reduce to twice the line tension η_{plan} of the corresponding single contact line on a planar substrate:

$$\begin{aligned} \eta(l_0 \rightarrow \infty) &= 2\sqrt{2\sigma_{lg}} \int_{l_\infty}^{\infty} dl \left\{ \sqrt{V(l \sin \varphi) - V(l_\infty \sin \varphi)} - \sqrt{\frac{\sigma_{lg}}{2}} \cos \varphi \right\} \\ &= 2\eta_{plan} + O\left(\left(\frac{1}{2}\pi - \varphi\right)^2\right) \end{aligned} \quad (3.15)$$

where within the present interface model η_{plan} is indeed given by [57]

$$\eta_{plan} = \sqrt{2\sigma_{lg}} \int_{l_\infty}^{\infty} dl \left\{ \sqrt{V(l) - V(l_\infty)} - \sqrt{-S} \right\} \quad (3.16)$$

with the spreading coefficient $S = \sigma_{wg} - \sigma_{lg} - \sigma_{wl} = -\sigma_{lg}(1 - \cos \Theta)$ equal to $-\frac{1}{2}\sigma_{lg} \cos^2 \varphi$ for $T = T_\varphi$. However, within a full theory one expects that $\eta(l_0 \rightarrow \infty) = 2\eta_{plan} + \eta_l$ where η_l is the line tension of a wedge filled with liquid, including the liquid phase as boundary condition in the bulk limit. But this latter contribution is not contained in the present *interface* model.

D. Phase diagram

In order to translate the general features of the line tension discussed in the previous subsection into an actual phase diagram one has to specify the functional form of the effective potential, i.e., $\omega(L)$ (see Eq.(3.2)). In the spirit of the square gradient expression (Eq.(3.7)), which is applicable for systems with short-ranged forces [58], we choose the generic form obtained by Fisher and Jin [59]

$$\omega(L) = W \exp\left(-\frac{L}{\xi}\right) + U \left(1 - C W^2 \frac{L}{\xi}\right) \exp\left(-\frac{2L}{\xi}\right) + \Delta\mu \Delta\rho L . \quad (3.17)$$

Since at present we are aiming for the generic, possible features of the phase behavior in wedges we refrain from studying the specific effects due to an algebraic decay of $\omega(L \rightarrow \infty)$ as it is characteristic for actual fluids governed by dispersion forces [15]; this is left to future studies. In Eq.(3.17) ξ is the correlation length in the bulk of the wetting phase, i.e., the liquid phase.

For $C \leq 0$ Eq.(3.17) yields a continuous wetting transition at coexistence $\Delta\mu = 0$ if $W(T < T_w) < 0$, $W(T = T_w) = 0$, $W(T > T_w) > 0$, and $U(T_w) > 0$. In this case the phase diagram consists of the line of first-order gas-liquid bulk transitions at $\mu = \mu_0(T)$ and of the temperatures T_c , T_w , and T_φ as determined by Eq.(3.11) on that line corresponding to the bulk, surface, and line nonanalyticities, respectively. For $\mu \neq \mu_0(T)$ there are no nonanalyticities.

For $C > 0$, $W(T) > 0$, and $U > 0$ Eq.(3.16) describes a first-order wetting transition at $T = T_w$ due to a decrease of $W(T)$ for $T \nearrow T_w$ such that $W(T_w) = W_w(C, U) > 0$. For reasons of simplicity we take U , C , and ξ as constant and consider a linear temperature dependence of $W(T) = W_w + W_0(T_w - T)/T_w$, $W_0 > 0$. The chemical potential difference can be expressed in terms of the dimensionless variable $(\Delta\mu \Delta\rho \xi)/W_w$. Figure 8 illustrates the phase diagram predicted by this model. The thick lines indicate the bulk singularities at $\mu = \mu_0$, which for simplicity we have taken to be temperature independent, and the prewetting line emanating from T_w and ending at the prewetting critical point C_{pw} . The prewetting line $T_{pw}(\Delta\mu)$ (or $\Delta\mu_{pw}(T)$) joins the gas-liquid coexistence curve tangentially [60] such that $T_{pw}(\Delta\mu \rightarrow 0) - T_w \sim \Delta\mu \ln \Delta\mu$ in accordance with the exponential decay of $\omega(L \rightarrow \infty)$. On the present scale of Figs.8 and 9 this tangential approach is not visible. The first-order filling transition occurs at $T_\varphi < T_w$ such that T_φ approaches T_w for $\varphi \rightarrow \frac{1}{2}\pi$. This infinite jump from a microscopic filling height to a macroscopic height at coexistence is reduced to a finite discontinuity off coexistence $\mu < \mu_0$ forming a prefilling line $\mu_{pf}(T)$ which joins the gas-liquid coexistence curve also tangentially. From our numerical analysis we find

$\mu_{pf}(T \searrow T_\varphi) - \mu_0 \sim a(\Delta T)^2 + b(\Delta T)^4 + \dots$ with $\Delta T = T - T_\varphi$. The thin-thick jump of the filling height across the prefilling line diverges $\sim (\Delta\mu)^{-1}$ for $\mu \rightarrow \mu_0$ (see Eq.(3.12)) and vanishes upon approaching the prefilling critical point C_{pf} . For sufficiently narrow wedges the prefilling lines are completely below the prewetting line and shorter than the latter. Upon increasing the opening angle of the wedge the prefilling line slides into the prewetting line thereby breaking up into two pieces: one between T_φ and a so-called extraordinary point denoted as $E^{(1)}$ and another between a second extraordinary point $E^{(2)}$ and the prefilling critical point C_{pf} . In the limit $\varphi \rightarrow \frac{1}{2}\pi$ these two pieces shrink to zero, such that $E^{(1)} \rightarrow w$ and $E^{(2)} \rightarrow C_{pw}$. Figure 9 summarizes the type of the phase transitions in the meniscus shape of the liquid in the wedge across the various phase boundaries for a very wide wedge. Crossing the pieces of the prefilling line along the paths 1 and 2 leads to a discontinuous increase of the filling height of the wedge but does not change the thickness of the wetting layer far away from the center of the wedge. A subsequent crossing of the prewetting line leads to a discontinuous increase of the thickness of the wetting film and a discontinuous change of the meniscus profile $l(x)$ but such that – surprisingly – just the filling height $l_0 = l(x=0)$ increases continuously (paths 3 and 4). Along path 5 both the thickness of the wetting film and the filling height change discontinuously; that happens only upon crossing the prewetting line. According to Fig.9 for suitable model systems along an isotherm $\Delta\mu \rightarrow 0$ with a temperature $T_\varphi < T < T_w$ one observes a reentrant prefilling of the wedge. For large undersaturations the filling height is very small. It increases until the prefilling line connecting C_{pf} and $E^{(2)}$ is reached. Crossing it leads to a discontinuous decrease of the filling height upon decreasing $\Delta\mu$. A further decrease of $\Delta\mu$ leads again to an increase of the filling height which jumps to an even larger value upon crossing the prefilling line connecting the filling point f and the extraordinary point $E^{(1)}$. Once this prefilling line has been passed the filling height diverges continuously for $\Delta\mu \rightarrow 0$ (see Eq.(3.12)).

E. Fluctuations

Upon crossing the prefilling line the filling height l_0 jumps from a value $l_0^<$ to a larger

value $l_0^>$ so that a volume ΔV proportional to $\frac{1}{2}((l_0^>)^2 - (l_0^<)^2)L_0 \tan \varphi$ is transformed from gas into liquid; L_0 is the linear extension of the wedge in y direction. (The above expression corresponds to flat menisci at height $l_0^<$ and $l_0^>$, respectively.) Thus effectively $\Delta\rho\Delta V$ particles participate in this phase transition. Therefore in the thermodynamic limit $L_0 \rightarrow \infty$ only at coexistence, i.e., for the filling transition with $l_0^> = \infty$, this phase transition corresponds to a true two-dimensional system which can indeed support a phase transition at $T > 0$. However, along the prefilling line $l_0^>$ is finite so that in that case the system is quasi-one-dimensional and cannot undergo a true phase transition for realistic interaction potentials. Therefore we conclude that the prefilling lines, as predicted by the mean-field theory described in the previous subsections, are wiped out by fluctuations in space dimensions $d = 3$. Only the filling transitions *at* coexistence, which can be either continuous or first-order, are true phase transitions. These conclusions are in accordance with considering the critical points C_{pw} of the prewetting line and C_{pf} of the prefilling line (see Figs. 8 and 9). Whereas C_{pw} belongs to the Ising universality class in $d = 2$, C_{pf} would belong to the Ising universality class in $d = 1$ and thus cannot exist.

One can identify the type of fluctuations which wipe out the prefilling line. If it would exist, by imposing suitable boundary conditions at the two ends of the groove for thermodynamic states at the prefilling line one could generate a stable interface perpendicular to the y direction of the wedge which smoothly interpolates between a portion of the wedge filled up to $l_0^<$ and another portion filled up to $l_0^>$. However, in this quasi-one-dimensional system the fluctuations of the filling height l_0 along the y direction, which are not captured by mean-field theory, are so strong that for this thermodynamic state at the presumed prefilling line the interface configuration in the wedge breaks up into many domains with $l_0^>$ and $l_0^<$, respectively, whose positions fluctuate strongly.

However, close to liquid-vapor coexistence $l_0^>$ is very large so that overturning a $l_0^<$ -domain into a $l_0^>$ -domain and vice versa becomes increasingly improbable. Therefore at the prefilling line as function of T or μ the filling height $l_0(T, \mu)$ changes rapidly but smoothly between $l_0^>$ and $l_0^<$ such that along the prefilling line for $\mu \rightarrow \mu_0$, i.e., $l_0^> \rightarrow \infty$ this crossover

between $l_0^>$ and $l_0^<$ becomes steeper and is confined to a vanishingly narrow region around the prefilling line so that the true phase transition at the filling transition at coexistence is restored for $\Delta\mu \rightarrow 0$.

The width of this smooth transition region of $l_0(T, \mu)$ at the prefilling line can be estimated on the basis of the finite-size scaling theory for first-order phase transitions [61]. These results can be adapted to the present problem following the line of arguments in Sec.4 in Ref.[62] where the corresponding smearing out of the prewetting line on a cylindrical substrate of radius r_0 has been analyzed. Up to a pre-exponential factor, which depends inter alia on the details of the effective interface potential, the temperature range δT within which $l_0(T, \mu)$ crosses over smoothly from $l_0^>$ to $l_0^<$ is given by

$$\frac{\delta T}{T_\varphi} \sim \exp\left(-\frac{\bar{\kappa} \Sigma}{k_B T_\varphi}\right) , \quad (3.18)$$

where $\bar{\kappa}$ is a numerical factor of order unity and Σ is the energy required for the formation of a domain wall between a $l_0^>$ -domain and a $l_0^<$ -domain. As a crude estimation we approximate Σ by $2\sigma_{lg}(l_0^>)^2 \tan \varphi$. (Here the effective width $2l_0^> \tan \varphi$ of the wedge replaces the cylinder radius r_0 in Ref.[62]; as in Ref.[62] the line tension Σ_l introduced there is approximated by $l_0^> \sigma_{lg}$.) Since $\frac{\xi^2 \sigma_{lg}}{k_B T_\varphi}$ is of order unity [62], where ξ is the bulk correlation length, we finally arrive at the estimate

$$\frac{\delta T}{T_\varphi} \sim \exp\left(-\kappa \left(\frac{l_0^>}{\xi}\right)^2 \tan \varphi\right) . \quad (3.19)$$

As soon as $l_0^>$ becomes significantly larger than ξ the temperature region δT for the smooth crossover is vanishingly small. Since $l_0^>$ diverges as $(\Delta\mu)^{-1}$ for $\Delta\mu \rightarrow 0$ along the prefilling line we conclude that close to liquid-vapor coexistence the difference between a true first-order thin-thick transition for l_0 cannot be experimentally distinguished from the actual smooth but very steep crossover. In this sense the prefilling line as obtained by mean-field theory remains an experimentally accessible line of (quasi-)nonanalyticities. Only close to C_{pf} this smearing out of the prefilling line becomes effective. There, in Eq.(3.19) $l_0^>$ must be replaced by $l_0^> - l_0^<$.

IV. Meniscus shape

So far we have discussed the configuration in the wedge only in terms of its key characteristic feature, i.e., the filling height l_0 (see Subsec.IIIB). The more detailed information about the full meniscus shape requires to solve Eq.(3.3) or its approximate version given by Eqs.(3.8) and (3.9). Whereas the former typically requires a numerical solution, the implicit solution $l(x)$ of the latter reduces to an integration:

$$-\sqrt{\frac{1}{2}\sigma_{lg}} \sin \varphi \int_{l_0}^{l(x)} \frac{d\hat{l}}{\sqrt{V(\hat{l} \sin \varphi) - V(l_\infty \sin \varphi)}} = x \quad , \quad x > 0 \quad , \quad (4.1)$$

where l_0 is the equilibrium solution of Eq.(3.10) and $l(-x) = l(x)$. (Here and in the following we drop the overbar which indicates the minimum of Eq.(3.7).) For a given effective interface potential $V(L)$ Eq.(4.1) can readily be solved numerically.

For the model given in Eq.(3.17) it turns out that one can obtain *explicit* solutions for $C = 0$ and $\Delta\mu = 0$ describing a *critical wetting* transition of the corresponding planar substrate, i.e., $W = W_0(T_w - T)/T_w$ where here $W_0 < 0$ and $U > 0$. Within this model one has

$$l_\infty = \frac{\xi}{\sin \varphi} \ln \left(\frac{2U}{|W_0|t} \right) = \frac{\xi}{\sin \varphi} \ln \left(\sqrt{\frac{2U}{\sigma_{lg}}} \frac{1}{\cos \varphi} \frac{t_\varphi}{t} \right) \quad , \quad t = \frac{T_w - T}{T_w} \quad , \quad (4.2)$$

and

$$l_0 = l_\infty + \frac{\xi}{\sin \varphi} \ln \frac{t}{t - t_\varphi} \quad , \quad (4.3)$$

which diverges for $t \searrow t_\varphi$ where

$$t_\varphi = \frac{T_w - T_\varphi}{T_w} = \frac{\sqrt{2\sigma_{lg}U}}{|W_0|} \cos \varphi. \quad (4.4)$$

The contact angle is given by

$$\cos \Theta = 1 + \frac{\omega(l_\infty \sin \varphi)}{\sigma_{lg}} \quad . \quad (4.5)$$

which leads to (see Eq.(3.10))

$$1 - \cos \Theta = \frac{1}{2} \left(\frac{t}{t_\varphi} \right)^2 \cos^2 \varphi = \left(\frac{t}{t_\varphi} \right)^2 v(\varphi) \quad (4.6)$$

which is in accordance with Eq.(3.11) so that

$$\Theta(T_\varphi) = \left(\frac{1}{2} \pi - \varphi \right) \left[1 - \frac{1}{8} \left(\frac{1}{2} \pi - \varphi \right)^2 + O \left(\left(\frac{1}{2} \pi - \varphi \right)^4 \right) \right] . \quad (4.7)$$

For $x \geq 0$ the profile is determined by (see Eq.(3.9))

$$\sin \varphi \frac{dl(x)}{dx} = \sqrt{\frac{2U}{\sigma_{lg}}} \left(\frac{W}{2U} + \exp \left[-\frac{l(x)}{\xi} \sin \varphi \right] \right) \quad (4.8)$$

with the boundary condition $\frac{dl(x)}{dx} \Big|_{x=0^+} = -\cot \varphi$. The explicit solution of Eq.(4.8) can be written as

$$l(x) = l_\infty + \frac{\xi}{\sin \varphi} \ln \left(1 + \frac{1}{\frac{t}{t_\varphi} - 1} \exp \left[-\frac{t}{t_\varphi} \frac{x}{\xi} \cos \varphi \right] \right) , \quad x \geq 0 . \quad (4.9)$$

Equation (4.9) is in accordance with all expected limiting behaviors: $l(0) = l_0$ as given in Eq.(4.3); $t_\varphi \rightarrow 0$ for $\varphi \rightarrow \frac{1}{2}\pi$ (Eq.(4.4)) so that for x and t fixed $l(x) \rightarrow l_\infty$ which itself reduces to the planar value $l_\infty^{(p)} = \xi \ln \left(\frac{2U}{|W_0|t} \right)$ (Eq.(4.2)); and for large x the film thickness $l(x)$ approaches its asymptote exponentially from above:

$$l(x \rightarrow \infty) = l_\infty + \frac{\xi}{\sin \varphi} \frac{1}{\frac{t}{t_\varphi} - 1} e^{-\frac{t}{t_\varphi} \frac{x}{\xi} \cos \varphi} , \quad (4.10)$$

provided T is not too close to T_φ , i.e., $\frac{t}{t_\varphi} - 1 \gg \exp \left(-\frac{t}{t_\varphi} \frac{x}{\xi} \cos \varphi \right)$. For any fixed value of x the profile diverges for $t \rightarrow t_\varphi$ as (see Eq.(4.3))

$$l(x, t \rightarrow t_\varphi) = l_0 - \frac{\xi}{\sin \varphi} \frac{x}{\xi} \cos \varphi . \quad (4.11)$$

The maximum curvature, i.e., $l'''(x_0) = 0$ occurs at

$$\begin{aligned} x_0 &= \pm \frac{\xi}{\frac{t}{t_\varphi} \cos \varphi} \ln \left(\frac{1}{\frac{t}{t_\varphi} - 1} \right) \\ &= \pm \left(1 - \frac{t - t_\varphi}{t_\varphi} \right) (l_0 - l_\infty) \tan \varphi + O(t - t_\varphi) . \end{aligned} \quad (4.12)$$

Thus for $t \rightarrow t_\varphi$ the position of the maximum curvature is given by the intersection of the asymptote $f(x) = l_\infty + |x| \cot \varphi$ and the horizontal $z = l_0$. Figure 10 illustrates the change of the meniscus shape upon approaching the filling transition temperature t_φ .

The excess coverage Γ (see Fig.10) associated with the meniscus is given by

$$\Gamma = 2 \Delta \rho \int_0^\infty dx [l(x) - l_\infty] = \frac{4 \Delta \rho \xi^2}{\sin 2 \varphi} \frac{t_\varphi}{t} I \left(\frac{1}{\frac{t}{t_\varphi} - 1} \right) \quad (4.13)$$

with [63] $I(y) = \int_0^y dx x^{-1} \ln(1+x)$ (see Fig.11). Since $I(y \rightarrow \infty) = \frac{1}{6}\pi^2 + \frac{1}{2}\ln^2 y$ one finds that upon approaching the filling transition the excess coverage diverges as

$$\Gamma(t \rightarrow t_\varphi) = \frac{2 \Delta \rho \xi^2}{\sin 2 \varphi} \ln^2 \left(\frac{t}{t_\varphi} - 1 \right) . \quad (4.14)$$

For fixed temperature $\Gamma(\varphi \rightarrow \frac{1}{2}\pi)$ vanishes as $\frac{1}{2}\pi - \varphi$ (see Eq.(4.4) and $I(y \rightarrow 0) = y$).

The line tension associated with the meniscus shape is given by Eqs.(3.13), (3.14), (3.2), (3.17), and (4.2) - (4.4). One finds

$$\eta = -2 \xi \sigma_{lg} \left[1 + \left(\frac{t}{t_\varphi} - 1 \right) \ln \left(1 - \frac{t_\varphi}{t} \right) \right] \cot \varphi . \quad (4.15)$$

The line tension is negative and approaches its minimal value at $t = t_\varphi$ with a logarithmic singularity (see Fig.12) :

$$\eta(t \rightarrow t_\varphi) - \eta(t = t_\varphi) \sim - \left(\frac{t}{t_\varphi} - 1 \right) \ln \left(\frac{t}{t_\varphi} - 1 \right) . \quad (4.16)$$

For $\varphi \rightarrow \frac{1}{2}\pi$ (i.e., $t/t_\varphi \rightarrow \infty$) the line tension vanishes as

$$\eta \left(\frac{t}{t_\varphi} \rightarrow \infty \right) = -\xi \sigma_{lg} \left(\frac{t}{t_\varphi} \right)^{-1} \cot \varphi . \quad (4.17)$$

Thus for fixed temperature $\eta(\varphi \rightarrow \frac{1}{2}\pi)$ vanishes $\sim (\frac{1}{2}\pi - \varphi)^2$ (see Eq.(4.4)).

Finally it should be pointed out that in terms of the variable t/t_φ both the excess coverage Γ and the line tension η (see Eq.(4.15) and Fig.12) can be expressed by scaling functions which are independent of φ and the model parameters σ_{lg} , W_0 , and U . It will be interesting to see to which extent this feature is established by more realistic models.

V. Derivation of the effective interface Hamiltonian

The results presented in Secs. III and IV are based on the effective interface Hamiltonian $\mathcal{H}[f]$ given by Eq.(3.1). Although this expression for $\mathcal{H}[f]$ is rather plausible the status of this equation is that of a phenomenological ansatz. In this section we describe the derivation of Eq.(3.1) from a more basic model in order to justify our choice of $\mathcal{H}[f]$ and to gain insight into the limitations of this form of $\mathcal{H}[f]$.

For an actual fluid confined to a wedge the appropriate approach is to start from a density functional theory for the inhomogenous number density distribution incorporating the full substrate potential of the wedge and the dispersion forces between the fluid particles. However, here we refrain from this very demanding task of bridging the gap between a fully microscopic description on an atomic scale and $\mathcal{H}[f]$. Instead, by aiming at conceptual insight we focus on the less ambitious goal to derive $\mathcal{H}[f]$ from a suitably chosen Landau-Ginzburg-Wilson theory for an order parameter m which corresponds to the deviation of the mean local number density $\rho(\mathbf{r})$ of the fluid particles from the average bulk densities, i.e., $\rho(\mathbf{r}) = \frac{1}{2}(\rho_l + \rho_g) + m(\mathbf{r})$ such that $m < 0$ corresponds to a gaslike configuration and $m > 0$ to a liquidlike configuration. The values $m < 0$ (> 0) are favored by the conjugate field $h < 0$ (> 0). This bulk field is proportional to $\Delta\mu = \mu_0(T) - \mu$ such that for $h > 0$ there is the liquid phase whereas for $h < 0$ one has the gas phase. For the present wedge geometry (see Fig.1) the natural form of the *Landau-Ginzburg - Wilson* Hamiltonian is [64]

$$\mathcal{H}_{LGW}[m] = \int_{-\infty}^{\infty} dx \left\{ \int_{|x| \cot \varphi}^{\infty} dz \left(\frac{K}{2} \left[\left(\frac{\partial m(x, z)}{\partial z} \right)^2 + \left(\frac{\partial m(x, z)}{\partial x} \right)^2 \right] + \Phi(m(x, z)) + \frac{1}{\sin \varphi} \Phi_1(m(x), z = |x| \cot \varphi) \right) \right\} . \quad (5.1)$$

Here we have already assumed translational invariance in the y direction. $\Phi(m) = \Phi_0(m) - mh$ denotes the bulk free energy density. The bulk free energy density at coexistence $h = 0$, i.e., Φ_0 exhibits two equally deep minima located at $m_{\alpha 0} < 0$ and $m_{\beta 0} > 0$ corresponding to the gas (α) and liquid (β) densities, respectively. With the bulk phase being vapor we have either $h = 0^-$ at coexistence or $h < 0$ off coexistence. In the present context we employ the

so-called double-parabola model which is the simplest form of $\Phi_0(m)$ which allows one to obtain analytical results [59,65-67]:

$$\Phi_0(m) = \begin{cases} \frac{1}{2}K\xi_\alpha^{-2}(m - m_{\alpha 0})^2 & , m \leq 0 \\ \frac{1}{2}K\xi_\beta^{-2}(m - m_{\beta 0})^2 & , m \geq 0 \end{cases} \quad (5.2)$$

ξ_γ denotes the correlation length in the bulk phase $\gamma = \alpha, \beta$. The parameters are chosen such that $\Phi_0(m)$ is continuous at $m = 0$, i.e., $\xi_\alpha^{-1}m_{\alpha 0} = -\xi_\beta^{-1}m_{\beta 0}$. The term $-mh$ in $\Phi(m)$ can be absorbed into the double-parabola form as follows:

$$\Phi(m) = \begin{cases} \frac{1}{2}K\xi_\alpha^{-2}(m - m_{\alpha h})^2 + A_\alpha & , m \leq 0 \\ \frac{1}{2}K\xi_\beta^{-2}(m - m_{\beta h})^2 + A_\beta & , m \geq 0 \end{cases} \quad (5.3)$$

where $m_{\gamma h} = m_{\gamma 0} + h\xi_\gamma^2/K$ and $A_\gamma = -m_{\gamma 0}h - h^2\xi_\gamma^2/(2K)$ is the equilibrium bulk free energy density of the γ phase. Off coexistence, i.e., for $h < 0$ the α phase is the stable phase with $m_{\alpha h} = m_{\alpha 0} + h\xi_\alpha^2/K$ as the equilibrium value of the order parameter. The requirement of the occurrence of the metastable liquid phase, i.e., $m_{\beta h} > 0$ leads to the constraint $h > -K\xi_\beta^{-2}m_{\beta 0}$.

For the surface contribution in Eq.(5.1) we choose the common [64] expression

$$\Phi_1(m_1) = -h_1 m_1 - \frac{1}{2}g m_1 \quad (5.4)$$

where $m_1(x) = m(x, z = |x| \cot \varphi)$. The surface field h_1 is taken to be positive so that it has the opposite sign as h . It favors the liquid phase β near the wall whereas the bulk field h favors the vapor phase α . The surface enhancement parameter g is taken to be negative. In Eq.(5.1) the prefactor $\frac{1}{\sin \varphi}$ of the surface term takes into account the increase of the surface area as compared to its horizontal projection. In general the LGW-Hamiltonian can additionally contain a line contribution corresponding to the edge of the wedge as well as a modified surface term including lateral derivatives of the order parameter. Since it turns out that these contributions and modifications do not influence the filling transition temperature of the wedge we do not consider them here.

Following the approach of Fisher and Jin [59,66-68] we employ the so-called crossing criterion in order to construct the effective interface Hamiltonian corresponding to the type of interface configurations as depicted in Fig.1(b). Order parameter configurations $m(x, z)$, which are monotonic and compatible with the boundary conditions to be positive near the walls and negative in the bulk, exhibit a line $z = f(x)$ along which $m(x, z)$ is zero. The crossing criterion identifies this line as the position of the interface:

$$m(x, z = f(x)) = 0 . \quad (5.5)$$

The construction scheme for obtaining the effective interface Hamiltonian is to minimize Eq.(5.1) under the constraint of the boundary conditions and under the constraint given by Eq.(5.5) for a prescribed configuration $f(x)$. The resulting order parameter $\bar{m}(x, z; [f])$, which corresponds to this minimum and thus is a functional of $f(x)$, is inserted into Eq.(5.1) and yields as the surface contribution to \mathcal{H}_{LGW} the effective interface Hamiltonian $\mathcal{H}[f]$. The equilibrium shape $\bar{f}(x)$ of the meniscus minimizes $\mathcal{H}[f]$. (In the following we drop overbars.) $\frac{\delta \mathcal{H}_{LGW}[m]}{\delta m(x, z)} = 0$ yields (see Eq.(5.1))

$$K \left(\frac{\partial^2}{\partial x^2} + \frac{\partial^2}{\partial z^2} \right) m_\gamma(x, z) = \Phi'(m_\gamma(x, z)) , \quad (5.6)$$

and the boundary condition at the substrate

$$\begin{aligned} K \left(\frac{\partial m_\beta}{\partial z} - \text{sgn}(x) \cot \varphi \frac{\partial m_\beta}{\partial x} \right) \Big|_{z=|x|\cot\varphi} &= \frac{1}{\sin \varphi} \Phi'_1(m_\beta) \Big|_{z=|x|\cot\varphi} \\ &= - \frac{h_1 + g m_\beta}{\sin \varphi} \Big|_{z=|x|\cot\varphi} \end{aligned} \quad (5.7)$$

supplemented by the bulk boundary condition

$$\lim_{z \rightarrow \infty} m_\alpha(x, z) = m_{\alpha h} . \quad (5.8)$$

The indices α, β , and $\gamma = \alpha, \beta$ indicate that in the special case of the double-parabola model, which will be considered henceforth, either the upper or lower part of Eq.(5.3) must be used depending on the sign of m ; α corresponds to $m < 0$ and β corresponds to $m > 0$. In

Eq.(5.7) we have used the index β assuming that m is positive near the wall; otherwise the concept of an interface description would not be applicable.

Following Refs.[66] and [67] the solution of Eqs.(5.5)-(5.8) is expanded into a series of terms which contribute increasing orders of derivatives of $l(x) = f(x) - |x| \cot \varphi$:

$$m_\gamma = m_{\gamma\pi} + m_{\gamma 1} + m_{\gamma 2} + \dots \quad (5.9)$$

where the index π indicates the planar limit $2\varphi = \pi$. For the individual terms one obtains within the double-parabola model (Eq.(5.3))

$$m_{\gamma\pi} = m_{\gamma 0} + F_{\gamma 0}(z - |x| \cot \varphi, l(x)) , \quad (5.10)$$

$$m_{\gamma 1} = F_{\gamma 1}(z - |x| \cot \varphi, l(x)) \frac{dl(x)}{dx} , \quad (5.11)$$

and

$$m_{\gamma 2} = F_{\gamma 21}(z - |x| \cot \varphi, l(x)) \left(\frac{dl(x)}{dx} \right)^2 + F_{\gamma 22}(z - |x| \cot \varphi, l(x)) \frac{d^2 l(x)}{dx^2} . \quad (5.12)$$

The functions $F_{\gamma i}$ and $F_{\gamma 2i}$ depend on the lateral coordinate x only via the vertical distance $z - |x| \cot \varphi$ from the walls and via the local film thickness $l(x)$ but not separately. We note that due to the cusp nonanalyticity of $l(x)$ at $x = 0$ the higher order terms in Eq.(5.9) contain distributions which are singular at $x = 0$ (see, e.g., Eq.(5.12)). Since $m(x, z)$ is smooth for $z \neq f(x)$ (see Eqs.(5.3) and (5.5)) these singularities have to cancel each other in Eq.(5.9). Since in the following we focus on the lowest terms we do not pursue this aspect further.

The function $F_{\gamma 0}(u, v)$ satisfies the differential equation

$$\left(\frac{1}{\sin^2 \varphi} \frac{\partial^2}{\partial u^2} - \xi_\gamma^{-2} \right) F_{\gamma 0}(u, v) = 0 \quad (5.13)$$

with the boundary condition

$$K \frac{\partial}{\partial u} F_{\beta 0}(u, l(x)) \Big|_{u=0} = - (h_1 + g m_{\beta 0} + g F_{\beta 0}(u = 0, l(x))) \sin \varphi . \quad (5.14)$$

Equations (5.13) and (5.14) together with Eq.(5.8) lead to the first contribution $m_{\gamma\pi}$ in Eq.(5.9) which does not depend on derivatives of $l(x)$:

$$m_{\alpha\pi}(x, z; [f]) = m_{\alpha 0} \left[1 - \exp \left(-\frac{z - f(x)}{\xi_\alpha} \sin \varphi \right) \right] \quad (5.15)$$

and

$$\begin{aligned} m_{\beta\pi}(x, z; [f]) = m_{\beta 0} + B_+ \exp \left(\frac{z - f(x)}{\xi_\beta} \sin \varphi \right) + \\ B_- \exp \left(-\frac{z - f(x)}{\xi_\beta} \sin \varphi \right) \end{aligned} \quad (5.16)$$

where the coefficients B_\pm are given as

$$B_+ = -\frac{m_{\beta 0} + \tau X}{1 - \mathcal{G} X^2} \quad (5.17)$$

and

$$B_- = \frac{\tau + \mathcal{G} m_{\beta 0} X}{1 - \mathcal{G} X^2} \quad (5.18)$$

with

$$X = \exp \left(-\frac{l(x)}{\xi_\beta} \sin \varphi \right) , \quad (5.19)$$

$$\tau = \frac{h_1 + g m_{\beta 0}}{K \xi_\beta^{-1} - g} , \quad (5.20)$$

and

$$\mathcal{G} = -\frac{K \xi_\beta^{-1} + g}{K \xi_\beta^{-1} - g} . \quad (5.21)$$

The remaining functions $F_{\gamma 1}(u, v)$, $F_{\gamma 21}(u, v)$, and $F_{\gamma 22}(u, v)$ satisfy the following equations:

$$\left(\frac{1}{\sin^2 \varphi} \frac{\partial^2}{\partial u^2} - \xi_\gamma^{-2} \right) F_{\gamma 1}(u, v) = 2 \cot \varphi \frac{\partial^2 F_{\gamma 0}(u, v)}{\partial u \partial v} , \quad (5.22)$$

$$\left(\frac{1}{\sin^2 \varphi} \frac{\partial^2}{\partial u^2} - \xi_\gamma^{-2} \right) F_{\gamma 21}(u, v) = 2 \cot \varphi \frac{\partial^2 F_{\gamma 1}(u, v)}{\partial u \partial v} - \frac{\partial^2 F_{\gamma 0}(u, v)}{\partial v^2} , \quad (5.23)$$

and

$$\left(\frac{1}{\sin^2 \varphi} \frac{\partial^2}{\partial u^2} - \xi_\gamma^{-2} \right) F_{\gamma 22}(u, v) = 2 \cot \varphi \frac{\partial F_{\gamma 1}(u, v)}{\partial u} - \frac{\partial F_{\gamma 0}(u, v)}{\partial v} . \quad (5.24)$$

For constructing the effective Hamiltonian up to square-gradient terms only the functions $F_{\gamma 0}$ and $F_{\gamma 1}$ are needed. The solution of Eq.(5.22) is proportional to $\cot \varphi$ and only the

square of $F_{\gamma 1}$ contributes to the effective Hamiltonian. The terms proportional to $F_{\gamma i}$, $i = 1, 21, 22$, vanish because these terms are linear in deviations from $m_{\gamma\pi}$ which itself minimizes the flat substrate Hamiltonian; thus the prefactors multiplying these deviations vanish. For a wedge with a wide opening angle, i.e., φ close to $\frac{1}{2}\pi$, one has $\cot\varphi \ll 1$ so that in the spirit, which led to Eq.(3.7), this contribution can be neglected here, too. Thus, the effective Hamiltonian is obtained by inserting $m_{\gamma\pi}$ as given by Eqs.(5.14)-(5.20) into the LGW-Hamiltonian (Eq.(5.1)). For a wide wedge only terms up to $\left(\frac{dl(x)}{dx}\right)^2$ are retained leading – after subtracting the surface contribution to the free energy – to

$$\mathcal{H}[l] = \int_{-\infty}^{\infty} dx \left\{ \frac{\sin\varphi}{2} \Sigma_{\alpha\beta}(l \sin\varphi) \left(\frac{dl(x)}{dx} \right)^2 + \chi_{\alpha\beta}(l(x) \sin\varphi) \frac{dl(x)}{dx} \cos\varphi + \frac{V(l(x) \sin\varphi) - V(l_\infty \sin\varphi)}{\sin\varphi} \right\} . \quad (5.25)$$

The coefficients $\Sigma_{\alpha\beta}$ and $\chi_{\alpha\beta}$ and the potential V are given by

$$\Sigma_{\alpha\beta}(l(x) \sin\varphi) = \frac{K}{\sin\varphi} \left[\int_{|x| \cot\varphi}^{f(x)} dz \left(\frac{\partial m_{\beta\pi}}{\partial l} \right)^2 + \int_{f(x)}^{\infty} dz \left(\frac{\partial m_{\alpha\pi}}{\partial l} \right)^2 \right] , \quad (5.26)$$

$$\chi_{\alpha\beta}(l(x) \sin\varphi) = -\frac{K}{\sin\varphi} \left[\int_{|x| \cot\varphi}^{f(x)} dz \frac{\partial m_{\beta\pi}}{\partial z} \frac{\partial m_{\beta\pi}}{\partial l} + \int_{f(x)}^{\infty} dz \frac{\partial m_{\alpha\pi}}{\partial z} \frac{\partial m_{\alpha\pi}}{\partial l} \right] , \quad (5.27)$$

and

$$\begin{aligned} V(l(x) \sin\varphi) = & \\ & \sin\varphi \int_{|x| \cot\varphi}^{f(x)} dz \left[\Phi(m_{\beta\pi}) - \Phi(m_{\alpha h}) + \frac{K}{2 \sin^2\varphi} \left(\frac{\partial m_{\beta\pi}}{\partial z} \right)^2 \right] \\ & + \sin\varphi \int_{f(x)}^{\infty} dz \left[\Phi(m_{\alpha\pi}) - \Phi(m_{\alpha h}) + \frac{K}{2 \sin^2\varphi} \left(\frac{\partial m_{\alpha\pi}}{\partial z} \right)^2 \right] \\ & + \Phi_1(m_{\beta\pi}(x, z = |x| \cot\varphi; [f])) . \end{aligned} \quad (5.28)$$

In Eqs.(5.26)-(5.28) the profiles $m_{\alpha\pi}$ and $m_{\beta\pi}$ are given by Eqs.(5.15) and (5.16), respectively, and $m_{\alpha h} = m_{\alpha 0} + h\xi_\alpha^2/K$ is the bulk value of the order parameter. The differentiation with respect to l is a differentiation with respect to $l(x)$ for any fixed value of x . The stiffness

coefficients $\Sigma_{\alpha\beta}$ and $\chi_{\alpha\beta}$ as well as the potential V turn out to have the same functional dependence on the thickness of the wetting film as for the corresponding planar substrate. Here they are evaluated at the local normal distance $l(x) \sin \varphi$ to the wall (see Fig.1(b)). For large thicknesses of the wetting film both stiffness coefficients $\Sigma_{\alpha\beta}$ and $\chi_{\alpha\beta}$ approach constant values which are the surface tension $\sigma_{\alpha\beta}$ in both cases. The term linear in $\frac{dl(x)}{dx}$, which is known from studies of wetting on corrugated substrates [67], is multiplied by $\cos \varphi$ and thus for a wide wedge it can be neglected as compared with the other two contributions in Eq.(5.25). Therefore we can conclude that the phenomenological ansatz for the effective Hamiltonian in Eq.(3.7) can be derived systematically from a more basic theory in the limit of a wide opening angle of the wedge. The derivation shows which kind of terms are left out by the ansatz in Eq.(3.7).

Moreover, the model parameters entering into Eq.(3.7) can be expressed in terms of those of the underlying LGW-Hamiltonian. Within the double-parabola model and the identifications $\alpha = g$ and $\beta = l$ one finds

$$\sigma_{\alpha\beta} = \frac{1}{2} K (\xi_{\beta}^{-1} m_{\beta 0}^2 + \xi_{\alpha}^{-1} m_{\alpha 0}^2) , \quad (5.29)$$

$$\sigma_{w\beta} = \frac{1}{2} K \xi_{\beta}^{-1} \tau^2 - h_1 (\tau + m_{\beta 0}) - \frac{1}{2} g (\tau + m_{\beta 0})^2 , \quad (5.30)$$

and

$$\begin{aligned} \omega(L) &= \frac{W \exp\left(-\frac{L}{\xi_{\beta}}\right) + U \exp\left(\frac{2L}{\xi_{\beta}}\right)}{1 - \mathcal{G} \exp\left(\frac{-2L}{\xi_{\beta}}\right)} \\ &= W \exp\left(-\frac{L}{\xi_{\beta}}\right) + U \exp\left(-\frac{2L}{\xi_{\beta}}\right) + O\left(\exp\left(-\frac{3L}{\xi_{\beta}}\right)\right) \end{aligned} \quad (5.31)$$

with

$$W = 2 K \xi_{\beta}^{-1} m_{\beta 0} \tau \quad (5.32)$$

and

$$U = K \xi_{\beta}^{-1} (\mathcal{G} m_{\beta 0}^2 + \tau^2) \quad (5.33)$$

(compare Eqs.(3.2) and (3.17)). According to Eqs.(5.20) and (5.32) W is negative at low temperatures, at which $m_{\beta 0} > 0$ is large, and vanishes at $\tau = 0$ for $m_{\beta 0} = h_1/|g|$ which is an implicit equation for the wetting transition temperature. For $|g| > K/\xi_{\beta}$ one has $U(\tau = 0) > 0$ and the model exhibits a critical wetting transition as studied in Sec.IV. Thus if in Eq.(5.31) $\omega(L)$ is truncated after the first two terms we fully recover the model analyzed in the previous section.

Finally we note that in the limit of a wedge with wide opening angle the resulting form of $\mathcal{H}[f]$ in Eq.(5.24) does not depend on the special choice of $\Phi(m)$ corresponding to the double-parabola model, i.e., Eq.(5.3) but holds for a general functional form $\Phi(m)$, which describes two-phase coexistence with a critical point. In that case Eq.(5.13) is replaced by

$$\frac{\partial^2}{\partial u^2} F_{\gamma 0}(u, v) = \Phi'(F_{\gamma 0}(u, v)) \sin^2 \varphi . \quad (5.34)$$

Moreover the fact, that in Eq.(5.3) the functions $\Sigma_{\alpha\beta}$, $\chi_{\alpha\beta}$, and V exhibit the same functional form as for the planar substrate, holds also for a general expression for $\Phi(m)$.

VI. Summary

We have obtained the following main results for the structure of a fluid exposed to a substrate forming a wedge with opening angle 2φ (Fig.1(a)):

1. A nonvolatile liquid spreads along the edge of the wedge if its contact angle Θ on the corresponding planar substrate is less than $\frac{1}{2}\pi - \varphi$ (see Fig.2 and Eq.(2.14)). A vapor bubble in a liquid spreads along the wedge if $\Theta > \frac{1}{2}\pi + \varphi$ (Eq.(2.20)). Theory of capillarity tells that $\Theta(T = T_{\varphi}) = \frac{1}{2}\pi - \varphi$ marks also the filling transition temperature T_{φ} of a wedge by a volatile liquid in equilibrium with its vapor reservoir (Subsec.IIB). At liquid-vapor coexistence of the bulk phases the wedge is completely filled by the liquid phase for $T > T_{\varphi}$ although $T_{\varphi} < T_w$ where T_w with $\Theta(T = T_w) = 0$ denotes the wetting transition temperature of the corresponding planar substrate; $T_{\varphi \rightarrow \frac{1}{2}\pi} = T_w$. The filling transition constitutes a nonanalyticity in the *surface contribution* to the free energy of the liquid confined by the wedge (Eq.(2.18)).

2. For $T < T_\varphi$ or off liquid-vapor coexistence the surfaces of the wedge are covered by a thin wetting film which requires a more detailed microscopic description, e.g., by an effective interface Hamiltonian $\mathcal{H}[f]$ for the shape $f(x)$ of the ensuing meniscus of the emerging liquid-vapor interface (see Eqs.(3.1) and (3.7) and Fig.1(b)). The interaction of this interface with the substrate is governed by the effective interface potential V (Eq.(3.2)). This description allows one to compute the *line contribution* to the free energy which determines the shape of the meniscus. Without specifying the explicit functional form of V the dependence of the filling height l_0 (Fig.1(b)) on temperature and deviation $\Delta\mu$ from two-phase coexistence can be discussed graphically (Figs.3 and 4). The filling transition at T_φ and $\Delta\mu = 0$ can be continuous or discontinuous; the order of the filling transition is the same as the order of the wetting transition of the corresponding planar substrate. Quite generally l_0 diverges $\sim (\Delta\mu)^{-1}$ upon approaching coexistence, i.e., $\Delta\mu \rightarrow 0$, for $T > T_\varphi$ (Eq.(3.12)).
3. By analyzing the line tension (Eqs.(3.13) and (3.14)) graphically (Figs.5-7) one finds that a first-order filling transition at coexistence, at which l_0 jumps from a microscopic value to a macroscopic one, is accompanied by a prefilling line extending into the vapor phase region of the bulk phase diagram (Fig.8). This prefilling line is the locus of nonanalyticities in the line tension; there the surface and bulk contributions to the free energy are analytic. Upon crossing the prefilling line the filling height undergoes a first-order thin-thick transition (Fig.9). The prefilling line joins the line $\Delta\mu = 0$ of the bulk coexistence tangentially. For increasing opening angles T_φ moves towards T_w . Accordingly the prefilling line slides into the prewetting line and breaks up into two pieces (Figs.8 and 9) giving rise to rich reentrant prefilling transitions. These general features are born out explicitly by model calculations based on a specific choice of the effective potential (Eq.(3.17)).
4. The prefilling transition as obtained from mean-field theory is smeared out by fluctuations of the local filling height along the edge of the wedge (Subsec.IIE). Instead

of the jump the mean filling height changes smoothly between a small value $l_0^<$ and a large value $l_0^>$ near the prefilling line. For small undersaturations $\Delta\mu$ the larger value diverges $\sim (\Delta\mu)^{-1}$ so that in this limit the temperature resolution required for distinguishing between the jump and the actual smooth crossover is experimentally not accessible (see Eq.(3.19)). Due to $l_0^>(\Delta\mu = 0) = \infty$ the filling transition at coexistence persists even in the strict sense. Thus for a system, which exhibits a first-order wetting transition in planar geometry, the prefilling line in a wedge should be detectable in experiments.

5. Whereas the thermodynamic behaviour of gross features such as the filling height l_0 and thus the filling transition itself can be obtained on rather general grounds, the determination of the actual meniscus shape requires model calculations based on explicit choices for the interface effective potential V . For short-ranged forces (see Eq.(3.17) with $C=0$) exhibiting a continuous wetting transition the meniscus shape (Eq.(4.9) and Fig.10), the excess coverage (Fig.11), and the line tension (Fig.12) can be obtained analytically. In terms of the reduced temperature variable $t/t_\varphi = (T_w - T)/(T_w - T_\varphi)$, within this model the excess coverage and the line tension are governed by scaling functions (Figs.11 and 12) which are independent of the opening angle φ and of potential parameters. The scaling functions are nonanalytic for $T \rightarrow T_\varphi$ (see Eqs.(4.14) and (4.16)).
6. In the limit of a wide opening angle φ the effective interface Hamiltonian $\mathcal{H}[f]$ (Eq.(3.7)) can be deduced from a Landau-Ginzburg-Wilson Hamiltonian (Eq.(5.1)). This derivation (Sec.V) points towards additional terms in $\mathcal{H}[f]$ which appear for smaller opening angles and which are not yet included in Eq.(3.7).

Acknowledgements : It is a pleasure for us to acknowledge helpful discussions and comments by T. Boigs, R. Evans, and T. Getta.

Appendix A: Constrained equilibrium in a nonsymmetric wedge

The analysis presented in Subsec.IIA can be repeated for a nonsymmetric wedge characterized by contact angles Θ_1 and Θ_2 on the left and right side of the wedge, respectively. Also in this case the liquid with constrained volume V forms a single spherical liquid-gas interface or a bridge. In each case the interface intersects the sides of the wedge at angles which are equal to the corresponding contact angles.

In the case of a single interface the radius R of the corresponding circle is

$$R = \sqrt{V} \left\{ \frac{\Theta_1 + \Theta_2 + 2\varphi - \pi}{2} - \left(\frac{\cos \Theta_1 - \cos \Theta_2}{2 \cos \varphi} \right)^2 \cot \varphi + \frac{\cos \Theta_1 \cos(\Theta_1 + \varphi) + \cos \Theta_2 \cos(\Theta_2 + \varphi)}{2 \sin \varphi} \right\}^{-\frac{1}{2}} \quad (\text{A1})$$

while the surface free energy difference between the filled and the nonfilled wedge is given by

$$\Delta F = \pm 2 \sigma_{lg} \sqrt{V} \left\{ \frac{\Theta_1 + \Theta_2 + 2\varphi - \pi}{2} - \left(\frac{\cos \Theta_1 - \cos \Theta_2}{2 \cos \varphi} \right)^2 \cot \varphi + \frac{\cos \Theta_1 \cos(\Theta_1 + \varphi) + \cos \Theta_2 \cos(\Theta_2 + \varphi)}{2 \sin \varphi} \right\}^{\frac{1}{2}} \quad (\text{A2})$$

where the upper sign corresponds to a convex and the lower sign to a concave interface. The interface becomes flat and ΔF vanishes at a temperature T_φ determined implicitly by

$$\Theta_1(T_\varphi) + \Theta_2(T_\varphi) + 2\varphi = \pi . \quad (\text{A3})$$

This temperature marks a filling phase transition for a nonsymmetric wedge if the constraint of a fixed volume is removed in favor of a grand canonical ensemble. At $T = T_\varphi$ both the filled and the nonfilled configuration have the same surface free energies, independent of the volume of the liquid.

A bridge configuration in a nonsymmetric wedge is possible as well. The common radius R of both interfaces is

$$R = \sqrt{V} \left\{ \Theta_1 + \Theta_2 - \pi - \frac{1}{2} (\sin 2\Theta_1 + \sin 2\Theta_2) \right\}^{-\frac{1}{2}} \quad (\text{A4})$$

while the free energy difference between the liquid bridge and the nonfilled wedge is given by

$$\Delta F = 4\sigma_{lg} V \left\{ \varphi + \left[\frac{\cos^2 \Theta_1 + \cos^2 \Theta_2}{2} - 2 \left(\frac{\cos \Theta_1 - \cos \Theta_2}{2 \cos \varphi} \right)^2 \right] \cot \varphi \right\} \times \left\{ \Theta_1 + \Theta_2 - \pi - \frac{1}{2} (\sin 2\Theta_1 + \sin 2\Theta_2) \right\}^{-\frac{1}{2}}. \quad (\text{A5})$$

The bridge configuration occurs provided the following condition is fulfilled:

$$\left(\frac{\cos \Theta_1 + \cos \Theta_2}{2 \sin \varphi} \right)^2 + \left(\frac{\cos \Theta_1 - \cos \Theta_2}{2 \cos \varphi} \right)^2 > 1. \quad (\text{A6})$$

For $\Theta_1 = \Theta_2$ these expressions reduce to those given in Sec.II. For the symmetric wedge the interface is concave if $\Theta + \varphi < \frac{1}{2}\pi$ and convex if $\Theta + \varphi > \frac{1}{2}\pi$. In the nonsymmetric case it is possible for an interface to be convex or concave or even form a bridge if $\Theta_1 + \varphi < \frac{1}{2}\pi$ and simultaneously $\Theta_2 + \varphi > \frac{1}{2}\pi$.

Appendix B: Expansions for a wide wedge

For a wide wedge the opening angle is close to π so that $\varphi = \frac{1}{2}\pi - \varepsilon$ with $\varepsilon \ll 1$. In this limit $\frac{df}{dx} \equiv f_x$ is small for all x so that the first part of the integrand in Eq.(3.1) can be expanded into powers of f_x^2 . In terms of $l_x = f_x - \cot \varphi$, $x \geq 0$ one has

$$\begin{aligned} \sqrt{1 + f_x^2} - \frac{1}{\sin \varphi} &= \frac{1}{\sin \varphi} \left\{ (1 + 2l_x \cos \varphi \sin \varphi + l_x^2 \sin^2 \varphi)^{\frac{1}{2}} - 1 \right\} \\ &= \frac{1}{\sin \varphi} \left\{ \frac{1}{2} l_x^2 \sin^2 \varphi + l_x \sin \varphi \cos \varphi + O(\varepsilon^4) \right\} \\ &= \frac{1}{\sin \varphi} \left\{ \frac{1}{2} f_x^2 \sin^2 \varphi - \frac{1}{2} \cos^2 \varphi + O(\varepsilon^4) \right\} \\ &= \frac{1}{2} \sin \varphi \left\{ f_x^2 - \cot^2 \varphi \right\} + O(\varepsilon^4) \end{aligned} \quad (\text{B1})$$

Here we have used the fact that $\cos \varphi = \sin \varepsilon = O(\varepsilon)$ and that $|l_x|$ is largest for $x = 0$ with $|l_x(x = 0)| = \cot \varphi = \tan \varepsilon$ so that $l_x = O(\varepsilon)$. This leads to Eq.(3.7). From a systematic point of view in the last line of Eq.(B1) the prefactor $\sin \varphi = \cos \varepsilon$ can be dropped and $\cot^2 \varphi$ can be replaced by ε^2 . However, it turns out that it is advantageous to keep the full form of these terms (see Eqs.(3.9) and (3.10)).

References

- [1] D. Andelman, J.F. Joanny, and M. O. Robbins, *Europhys. Lett.* **7**, 731 (1988); M. O. Robbins, D. Andelman, J. F. Joanny, *Phys. Rev. A* **43**, 4344 (1991); J. L. Harden and D. Andelman, *Langmuir* **8**, 2547 (1992).
- [2] P. Pfeifer, Y.J. Wu, M.W. Cole, and J. Krim, *Phys. Rev. Lett.* **62**, 1997 (1989); P. Pfeifer, M.W. Cole, and J. Krim, *Phys. Rev. Lett.* **65**, 663 (1990).
- [3] M. Kardar and J.O. Indekeu, *Phys. Rev. Lett.* **65**, 662 (1990); *Europhys. Lett.* **12**, 161 (1990); H. Li and M. Kardar, *Phys. Rev. B* **42**, 6546 (1990); J. Krim and J.O. Indekeu, *Phys. Rev. E* **48**, 1576 (1993).
- [4] E. Cheng, M.W. Cole, and A.L. Stella, *Europhys. Lett.* **8**, 537 (1989); E. Cheng, M.W. Cole, and P. Pfeifer, *Phys. Rev. B* **39**, 12962 (1989).
- [5] G. Giugliarelli and A.L. Stella, *Phys. Scripta T* **35**, 34 (1991); *Phys. Rev. E* **53**, 5035 (1996); *Physica A* **239**, 467 (1997); G. Sartoni, A.L. Stella, G. Giugliarelli, and M.R. D'Orsogna, *Europhys. Lett.* **39**, 633 (1997).
- [6] G. Palasantzas, *Phys. Rev. B* **48**, 14472 (1993); *Phys. Rev. B* **51**, 14612 (1995).
- [7] C. Borgs, J. De Coninck, R. Kotecký, and M. Zinque, *Phys. Rev. Lett.* **74**, 2293 (1995); K. Topolski, D. Urban, S. Brandon, and J. De Coninck, *Phys. Rev. E* **56**, 3353 (1997).
- [8] J.Z. Tang and J.G. Harris, *J. Chem. Phys.* **103**, 8201 (1995).
- [9] R. Netz and D. Andelman, *Phys. Rev. E* **55**, 687 (1997).
- [10] A.O. Parry, P.S. Swain, and J.A. Fox, *J. Phys.: Condens. Matter* **8**, L659 (1996); P.S. Swain and A.O. Parry, *J. Phys. A: Math. Gen.* **30**, 4597 (1997).
- [11] D. Beaglehole, *J. Phys. Chem.* **93**, 893 (1989).

[12] S. Garoff, E.B. Sirota, S.K. Sinha, and H.B. Stanley, *J. Chem. Phys.* **90**, 7505 (1989).

[13] I. M. Tidswell, T.A. Rabedeau, P.S. Pershan, and S.D. Kosowsky, *Phys. Rev. Lett.* **66**, 2108 (1991), P.S. Pershan, *Ber. Bunsenges. Phys. Chem.* **98**, 372 (1994).

[14] V. Panella and J. Krim, *Phys. Rev. E* **49**, 4179 (1994).

[15] S. Dietrich, in *Phase Transitions and Critical Phenomena*, edited by C. Domb and J.L. Lebowitz (Academic, London, 1988), Vol.12, p. 1.

[16] M. Schick, in *Liquids at Interfaces, Proceedings of the Les Houches Summer School in Theoretical Physics, Session XLVIII*, edited by J. Chavrolin, J. F. Joanny, and J. Zinn-Justin (North-Holland, Amsterdam, 1990), p. 415.

[17] W. Hansen, J.P. Kotthaus, and U. Merkt, in *Semiconductors and Semimetals*, edited by M. Reed (Academic, London, 1992), Vol. 35, p. 279.

[18] P. Bönsch, D. Wüllner, T. Schrimpf, A. Schlachetzki, and R. Lacmann, *J. Electrochem. Soc.* **145**, 1273 (1998).

[19] D.W.L. Tolfree, *Rep. Prog. Phys.* **61**, 313 (1998).

[20] J.A. Mann, Jr., L. Romero, R.R. Rye, and F.G. Yost, *Phys. Rev. E* **52**, 3967 (1995); R.R. Rye, F.G. Yost, and J.A. Mann, *Langmuir* **12**, 555 (1996); *ibid* 4625 (1996).

[21] S. Gerdes and G. Ström, *Colloids and Surfaces A* **116**, 135 (1996); S. Gerdes, A.-M. Cazabat, and G. Ström, *Langmuir* **13**, 7258 (1997).

[22] M. Dong, F.A. Dullien, and I. Chatzis, *J. Coll. Interf. Sci.* **172**, 21 (1995); M. Dong and I. Chatzis, *J. Coll. Interf. Sci.* **172**, 278 (1995); D. Zhou, M. Blunt, and F.M. Orr, Jr., *J. Coll. Interf. Sci.* **187**, 11 (1997).

[23] E. Kim and G.M. Whitesides, *J. Phys. Chem. B* **101**, 855 (1997).

[24] J.B. Knight, A. Vishwanath, J. P. Brody, and R.H. Austin, Phys. Rev. Lett. **80**, 3863 (1998).

[25] M. Trau, N. Yao, E. Kim, Y. Xia, G.M. Whitesides, and I.A. Aksay, Nature **390**, 674 (1997).

[26] T.A. Winterningham, H.P. Gillis, D.A. Choutov, K.P. Martin, J. T. Moore, and K. Douglas, Surf. Sci. **406**, 221 (1998).

[27] F. Burmeister, C. Schäfle, B. Keilhofer, C. Bechinger, J. Boneberg, and P. Leiderer, Adv. Mater. **10**, 495 (1998).

[28] B.V. Derjaguin and N.V. Churaev, J. Coll. Inter. Sci. **54**, 157 (1976).

[29] J.R. Philip, J. Chem. Phys. **66**, 5069 (1977); *ibid* **67**, 1732 (1977).

[30] Y. Pomeau, J. Coll. Interf. Sci. **113**, 5 (1985).

[31] E. Cheng and M.W. Cole, Phys. Rev. B **41**, 9650 (1990).

[32] P.M. Duxbury and A.C. Orrick, Phys. Rev. B **39**, 2944 (1989).

[33] M. Napiórkowski, W. Koch, and S. Dietrich, Phys. Rev. A **45**, 5760 (1992).

[34] E.H. Hauge, Phys. Rev. A **46**, 4944 (1992).

[35] G.A. Darbellay and J. Yeomans, J. Phys. A: Math. Gen. **25**, 4275 (1992).

[36] E. Cheng, J.R. Banavar, M.W. Cole, and F. Toigo, Surf. Sci. **261**, 389 (1992).

[37] Y. Song, Phys. Lett. A **180**, 3611 (1993).

[38] A. Korociński and M. Napiórkowski, Mol. Phys. **84**, 171 (1995).

[39] M. Kagan, W. V. Pinczewski, and P. E. Oren, J. Coll. Interf. Sci. **170**, 426 (1995).

[40] M. Schoen and S. Dietrich, Phys. Rev. E **56**, 499 (1997).

- [41] D. Henderson, S. Sokołowski, and D. Wasan, Phys. Rev E **57**, 5539 (1998).
- [42] A. Lipowski, Phys. Rev. E **58**, R1 (1998).
- [43] P. Müller-Buschbaum, M. Tolan, W. Press, F. Brinkop, and J.P. Kotthaus, Ber. Bunsenges. Phys. Chem. **98**, 413 (1994).
- [44] Z. Li, M. Tolan, T. Höhr, D. Kharas, S. Qu, J. Sokolov, M.P. Rafailovich, H. Lorenz, J.P. Kotthaus, J. Wang, S.K. Sinha, and A. Gibaud, Macromolecules **31**, 1915 (1998).
- [45] For an overview of adsorption of fluids on structured substrates see S. Dietrich, in Proceedings of the NATO-ASI *New Approaches to Old and New Problems in Liquid State Theory - Inhomogeneities and Phase Separation in Simple, Complex and Quantum Fluids* held at Patti Marina (Messina), Italy, July 7-17, 1998, edited by C. Caccamo (Kluwer, Dordrecht), in press.
- [46] I.M. Gelfand and S.V. Fomin, *Calculus of Variations* (Prentice-Hall, Englewood Cliffs, 1963), Sec. 14.
- [47] T. Onda, S. Shibuichi, N. Satoh, and K. Tsujii, Langmuir **12**, 2125 (1996); S. Shibuichi, T. Onda, N. Satoh, and K. Tsujii, J. Phys. Chem. **100**, 19512 (1996).
- [48] J.K. Lee and H.I. Avronson, Surf. Sci. **47**, 692 (1975).
- [49] R.K.P. Zia, J.E. Avron, and J.E. Taylor, J. Stat. Phys. **50**, 727 (1988).
- [50] D. Langbein, J. Fluid Mech. **213**, 251 (1990).
- [51] J. De Coninck, J. Fruttero, and A. Ziermann, Physica A **196**, 320 (1993); *ibid* **199**, 243 (1993).
- [52] L.-H. Tang and Y. Tang, J. Phys. II France **4**, 881 (1994).
- [53] P. Concus and R. Finn, Phys. Fluids **10**, 39 (1998).

[54] S. Dietrich, in *Phase Transitions in Surface Films 2*, Proceedings of the NATO-ASI (Series B) held in Erice, Italy, 19-30 June 1990, edited by H. Taub, G. Torzo, H.J. Lauter, and S.C. Fain, Vol. B **267**, 391 (1991).

[55] S. Dietrich and M. Napiórkowski, Phys. Rev. A **43**, 1861 (1991).

[56] M. Kagan and W.V. Pinczewski, J. Coll. Interf. Sci. **203**, 379 (1998).

[57] J. O. Indekeu, Physica A **183**, 439 (1992); Int. J. Mod. Phys. B **8**, 309 (1994).

[58] S. Dietrich and M. Napiórkowski, Physica A **177**, 437 (1991); M. Napiórkowski and S. Dietrich, Z. Phys. B **89**, 263 (1992); Phys. Rev. E **57**, 1836 (1993); Z. Phys. B **97**, 511 (1995).

[59] M.E. Fisher and A.J. Jin, Phys. Rev. B **44**, 1430 (1991); Phys. Rev. Lett. **69**, 792 (1992); A.J. Jin and M.E. Fisher, Phys. Rev. B **47**, 7365 (1993); *ibid* **48**, 2642 (1993).

[60] E.H. Hauge and M. Schick, Phys. Rev. B **27**, 4288 (1983); M.P. Nightingale, W.F. Saam, and M. Schick, Phys. Rev. B **30**, 3830 (1984).

[61] V. Privman and M.E. Fisher, J. Stat. Phys. **33**, 385 (1983); J. Appl. Phys. **57**, 3327 (1985).

[62] T. Bieker and S. Dietrich, Physica A **252**, 85 (1998); due to a printer's error in Eq.(4.6) of this reference \sum_s should read \sum_l .

[63] $I(y) = -Li_2(-y)$ can be expressed in terms of the dilogarithmic function $Li_2(z) = -\int_0^z dz z^{-1} \ln(1-z)$. See L. Levin, *Polylogarithms and Associated Functions* (North Holland, New York, 1981) and L. Levin (ed.), in *Mathematical Surveys and Monographs*, Vol. 37, *Structural Properties of Polylogarithms* (American Mathematical Society, Providence, 1991).

[64] H.W. Diehl, in *Phase Transitions and Critical Phenomena*, edited by C. Domb and J.L. Lebowitz (Academic, London, 1986), Vol. 10, p. 76.

- [65] R. Lipowsky, *Z. Phys. B* **55**, 345, (1984).
- [66] K. Rejmer and M. Napiórkowski, *Z. Phys. B* **97**, 293 (1995).
- [67] K. Rejmer and M. Napiórkowski, *Z. Phys. B* **102**, 101 (1997).
- [68] M.E. Fisher, A.J. Jin, and A.O. Parry, *Ber. Bunsenges. Phys. Chem.* **98**, 357 (1994).

Figure captions

FIG.1.(a) Macroscopic description of a wedge with opening angle 2φ formed by identical walls whose surfaces are located at $z = |x| \cot \varphi$. The shape of the meniscus is described by $z = f(x)$ or $l(x) = f(x) - |x| \cot \varphi$. The liquid-gas interface intersects the walls at $x = \pm x_1$ with a contact angle Θ . The system is taken to be two-dimensional and its height is cut off at $z = H_0$. (b) Same as in (a) on a microscopic scale which takes into account that far away from the center of the wedge the meniscus reduces to a wetting film of thickness $l_\infty \sin \varphi$ covering the walls at large $|x|$; $l_\infty = l(x \rightarrow \infty)$. $l_0 \equiv l(x = 0)$ denotes the filling height of the liquid in the wedge.

FIG.2. Classification of the equilibrium shapes of a nonvolatile liquid drop (shaded area) as function of the opening angle 2φ of a symmetric wedge and of the contact angle Θ . In all cases the shape of the liquid-vapor interface is a part of a circle. The space within the wedge, which is not filled by the liquid, is occupied by vapor. Here the wedge is two-dimensional resembling the situation in which a three-dimensional system exhibits translational invariance along the edge of the wedge.

FIG.3. Schematic graphical solution for the filling height l_0 according to Eqs.(3.5) and (3.10), respectively, for the case of a critical wetting transition of the corresponding planar substrate, i.e., $\Delta\mu = 0$. In this case ΔV exhibits a single minimum at $l = l_\infty$ which moves smoothly to infinity for $T \rightarrow T_w$ and becomes more shallow for increasing temperature. For $l \rightarrow \infty$ the ratio $\Delta V/\sigma_{lg}$ attains the limiting value $1 - \cos \Theta(T)$ which vanishes for $T \rightarrow T_w$. By construction ΔV is positive. The intersection with the straight line $v(\varphi)$ yields the filling height l_0 . There are two solutions $l_0^{(1)}$ and $l_0^{(2)}$ but only the solution $l_0 > l_\infty$ is compatible with the boundary condition associated with Eq.(3.9) (see Subsec.IIC). For $T \nearrow T_\varphi$ the asymptote $1 - \cos \Theta(T)$ approaches $v(\varphi)$ from above so that l_0 diverges continuously for $T \nearrow T_\varphi$.

FIG.4. Same as Fig.3 for the case of a first-order wetting of the corresponding planar substrate. For $T \nearrow T_\varphi$ the difference $1 - \cos \Theta(T)$ reaches $v(\varphi)$ and l_0 increases smoothly to a finite maximum value $l_0^{(m)}$ at $T = T_\varphi$. At T_φ there is another solution $l_0 = \infty$. As will be shown in Subsec.IIIC, $l_0 = \infty$ is the thermodynamically stable solution for $T > T_\varphi$. Therefore at T_φ the filling height l_0 jumps from the finite value $l_0^{(m)}$ to infinity.

FIG.5. Schematic graphical interpretation of the line tension in the case of critical wetting of the corresponding planar substrate below (a) and at (b) the filling transition temperature. According to Eqs.(3.13) and (3.14), for $l_0 = l_0^{(1)}$ the line tension η is proportional to the vertically hatched area A , which is to be taken negatively, whereas for $l = l_0^{(2)}$ the line tension η is proportional to the horizontally hatched area, which is to be taken positively. Therefore $l_0^{(1)}$ has the lower line tension and is thermodynamically stable. For $T \nearrow T_\varphi$ l_∞ increases, the minimum of $\sqrt{\Delta V}$ becomes less steep, and $l_0^{(1)}$ moves out to infinity corresponding to the filling of the wedge. Even for dispersion forces with $V(L \rightarrow \infty) \sim L^{-2}$ the area A and the line tension η remain finite for $T \nearrow T_\varphi$. The second value of l_0 , i.e., $l_0^{(2)}$ does not correspond to solution of Eq.(3.4) or (3.9).

FIG.6. Same as Fig.5 for first-order wetting of the corresponding planar substrate. For $T \nearrow T_\varphi$ both l_∞ and l_0 increase but stay finite. At T_φ the filling height $l_0 = \infty$ is also a solution, but the corresponding line tension is larger than that corresponding to the indicated finite solution by an amount given by the horizontally hatched area, which is to be taken positively. For $T > T_\varphi$ the surface free energy favors the filled wedge so that $l_0(T)$ undergoes a discontinuous jump from a finite value at $T = T_\varphi^-$ to a macroscopically large value at T_φ^+ .

FIG.7. Schematic illustration of the filling transition of the wedge along isotherms $\Delta\mu \rightarrow 0$ above the filling temperature T_φ for critical (a) and first-order wetting (b) of the correspond-

ing planar substrate. Off coexistence $\sqrt{\Delta V/\sigma_{lg}}$ increases for large l as $(\Delta\mu\Delta\rho\sin\varphi/\sigma_{lg})^{\frac{1}{2}}l^{\frac{1}{2}}$ whereas $\sqrt{\Delta V/\sigma_{lg}}$ attains the finite value $\sqrt{1-\cos\Theta}$ for $\Delta\mu=0$ which is less than $\sqrt{v(\varphi)}$ for $T>T_\varphi$. In the case of critical wetting there is a single filling height l_0 which can possibly be thermodynamically stable. For $\Delta\mu\rightarrow 0$ the wetting film thickness l_∞ increases slightly but remains finite whereas l_0 diverges continuously. The vertically hatched area diverges also so that $\eta(\Delta\mu\rightarrow 0, T>T_\varphi)\rightarrow -\infty$. In the case of first-order wetting $\sqrt{\Delta V/\sigma_{lg}}$ exhibits a global minimum at $l_\infty^{(1)}$ and a local minimum at $l_\infty^{(2)}$. Upon crossing the prewetting line of the corresponding planar substrate $l_\infty^{(2)}$ turns into the global minimum. Thus (b) corresponds to a case $T_w>T>T_\varphi$. For large $\Delta\mu$ the area $|A_3|=-A_3$ is smaller than $A_2>0$ so that $A_2+A_3>0$. Consequently $l_0^{(1)}$ corresponds to the global minimum of the line tension. For $\Delta\mu\rightarrow 0$ the area $|A_3|$ increases without limit so that there is a critical value $\Delta\mu_{pf}(T)$ at which $|A_3|=A_2$ so that for $\Delta\mu<\Delta\mu_{pf}(T)$ the filling height $l_0^{(2)}$ becomes the globally stable configuration. Upon lowering $\Delta\mu$ further $l_0^{(2)}$ diverges, as well as $A_1+A_2+A_3$, leading to the filling of the wedge. For reasons of clarity we have ignored the slight changes in $\sqrt{\Delta V/\sigma_{lg}}$ for $l\leq l_\infty^{(2)}$ upon lowering $\Delta\mu$. $\Delta\mu_{pf}(T)$ marks a prefilling transition in the wedge.

FIG.8. (a) Phase diagram for the filling of a wedge in the case that the corresponding planar substrate exhibits a first-order wetting transition at T_w . The thick phase boundaries represent the gas-liquid coexistence curve at $\mu=\mu_0$, which for reasons of simplicity has been taken to be a straight line, and the prewetting line emanating from T_w and ending at a prewetting critical point C_{pw} . The bulk critical point T_c is off the scale to the right. We use dimensionless quantities $\mu^*-\mu_0^*=-\Delta\mu\Delta\rho\xi/W_w$ (see the main text) and $T^*=T/T_w$ so that $T_w^*=1$. The temperatures T_{φ_i} denote first-order filling transition temperatures which move towards T_w for increasing values of φ_i . From each filling transition point a so-called prefilling line emanates ending in a critical prefilling point C_{pf} . The prefilling lines join the gas-liquid coexistence line tangentially as a quadratic function whereas the corresponding tangential approach of the prewetting line is logarithmic and

not visible on the present scale. For $\varphi \rightarrow \frac{1}{2}\pi$ the prefilling line touches the prewetting line and breaks into two pieces. For $\varphi = \varphi_3$ in (a) the lower piece between the extraordinary point $E_3^{(2)}$ and C_{pf} is shown. On this scale the upper piece between T_{φ_3} and $E_3^{(1)}$ is not visible as well as the distinction between T_w and T_{φ_3} . This is resolved in (b) on a magnified scale. These phase diagrams have been obtained for the model defined by Eqs.(3.7), (3.10), (3.2), and (3.17) using the following potential parameters: $C/W_w^2 = 3.504823$, and $U/W_w = 0.197338$. For the angles $\varphi_1 = 81.40^\circ$, $\varphi_2 = 83.12^\circ$, $\varphi_3 = 84.84^\circ$, $\varphi_4 = 85.99^\circ$, and $\varphi_5 = 87.13^\circ$ with $W_{\varphi_i} = W(T_{\varphi_i})$ one obtains $W_{\varphi_1}/W_w = 1.008580$, $W_{\varphi_2}/W_w = 1.005532$, $W_{\varphi_3}/W_w = 1.003130$, $W_{\varphi_4}/W_w = 1.001899$, and, $W_{\varphi_5}/W_w = 1.000971$ so that $T_w^* - T_{\varphi_i}^* = \frac{W_w}{W_0} \left(\frac{W_{\varphi_i}}{W_w} - 1 \right)$. Putting numbers on the axis requires to choose a value for the ratio $\frac{W_w}{W_0}$. For $\frac{W_w}{W_0} = 1$ one obtains $T_w^* - T_{\varphi_i}^* = 0.008580, 0.005532, 0.003130, 0.001899, 0.000971$, for $i=1,\dots,5$ and $T_{C_{pw}}^* = 1.594132$ and $\mu^*(T_{C_{pw}}) - \mu_0^* = -0.038024$. For a different value of $\frac{W_w}{W_0}$ the temperatures are rescaled linearly according to the formula given above.

FIG.9. Types of morphology of the wetting film in a wedge for the various phases within a schematic phase diagram. The notation is the same as in Fig.8. The opening angle φ is sufficiently large so that the prefilling line is split into two pieces forming the two extraordinary points $E^{(1)}$ and $E^{(2)}$. Along the thermodynamic paths 1 and 2 the filling height l_0 in the center of the wedge increases discontinuously upon crossing the pieces of the prefilling line but the thickness l_∞ of the wetting film far away from the center of the wedge does not jump. Along the thermodynamic paths 3 and 4 l_∞ increases discontinuously while l_0 grows smoothly upon crossing the prewetting line. Along the thermodynamic path 5 both l_0 and l_∞ jump only at the prewetting line.

FIG.10. Shape $f(x) = f(-x)$ of the meniscus in units of the bulk correlation length ξ in the liquid phase. $f(x > 0) = l(x) + x \cot \varphi$ with $l(x)$ given by Eqs.(4.2) and (4.9). The planar substrate undergoes a critical wetting transition at T_w . The temperature is raised towards the filling transition temperature T_φ , i.e., $t/t_\varphi = (T_w - T)/(T_w - T_\varphi) \rightarrow 1$ along

two-phase coexistence in the bulk. In units of ξ and in terms of t/t_φ the profile is determined uniquely by the dimensionless parameter $\sqrt{2U/\sigma_{lg}}$ which is chosen to be 2 here. The diamonds indicate the position of the maximum curvature of $f(x)$. As explained in the main text this position attains a constant distance from the wall for $t/t_\varphi \rightarrow 1$. The shaded area corresponds to half of the wedge excess coverage $\Gamma/\Delta\rho$ (see Eq.(4.13)) for $t/t_\varphi = 10^{-2}$. The dotted line indicates the asymptote of $f(x)$ extended to $x = 0$. At the present scale the temperature dependence of the asymptotes, i.e., of l_∞ is not visible.

FIG.11. Inverse of the reduced excess coverage $\Gamma^* = \Gamma(\sin(2\varphi))/(4\Delta\rho\xi^2)$ as function of reduced temperature t/t_φ (Eq.(4.13)). Upon approaching the filling transition temperature Γ^* diverges $\sim \ln^2(t/t_\varphi - 1)$ (see Eq.(4.14) and the inset). For $\varphi \rightarrow \frac{1}{2}\pi$, i.e., $t/t_\varphi \rightarrow \infty$ the inverse coverage $1/\Gamma^*$ diverges quadratically so that $\Gamma \sim \Gamma^*/\sin(2\varphi) \sim \varphi - \frac{1}{2}\pi$ for $\varphi \rightarrow \frac{1}{2}\pi$, i.e., $t/t_\varphi \rightarrow \infty$. Note that in terms of the variable t/t_φ the functional form of Γ^* is independent of φ and the model parameters σ_{lg} , W_0 , and U .

FIG.12. Reduced line tension $\eta^* = \eta/(2\xi\sigma_{lg}\cot\varphi)$ as function of t/t_φ (Eq.(4.15)). η^* is negative and attains its minimum at $t = t_\varphi$ in a cusplike singularity $\sim (t/t_\varphi - 1)\ln(t/t_\varphi - 1)$ (Eq.(4.16)). For $\varphi \rightarrow \frac{1}{2}\pi$, i.e., $t/t_\varphi \rightarrow \infty$, the line tension η^* vanishes as $-\frac{1}{2}t/t_\varphi$ so that $\eta \sim \eta^*\cot\varphi \sim (\varphi - \frac{1}{2}\pi)^2$ for $\varphi \rightarrow \frac{1}{2}\pi$. In terms of the variable t/t_φ the functional form of η^* is independent of φ and the model parameters σ_{lg} , W_0 , and U .

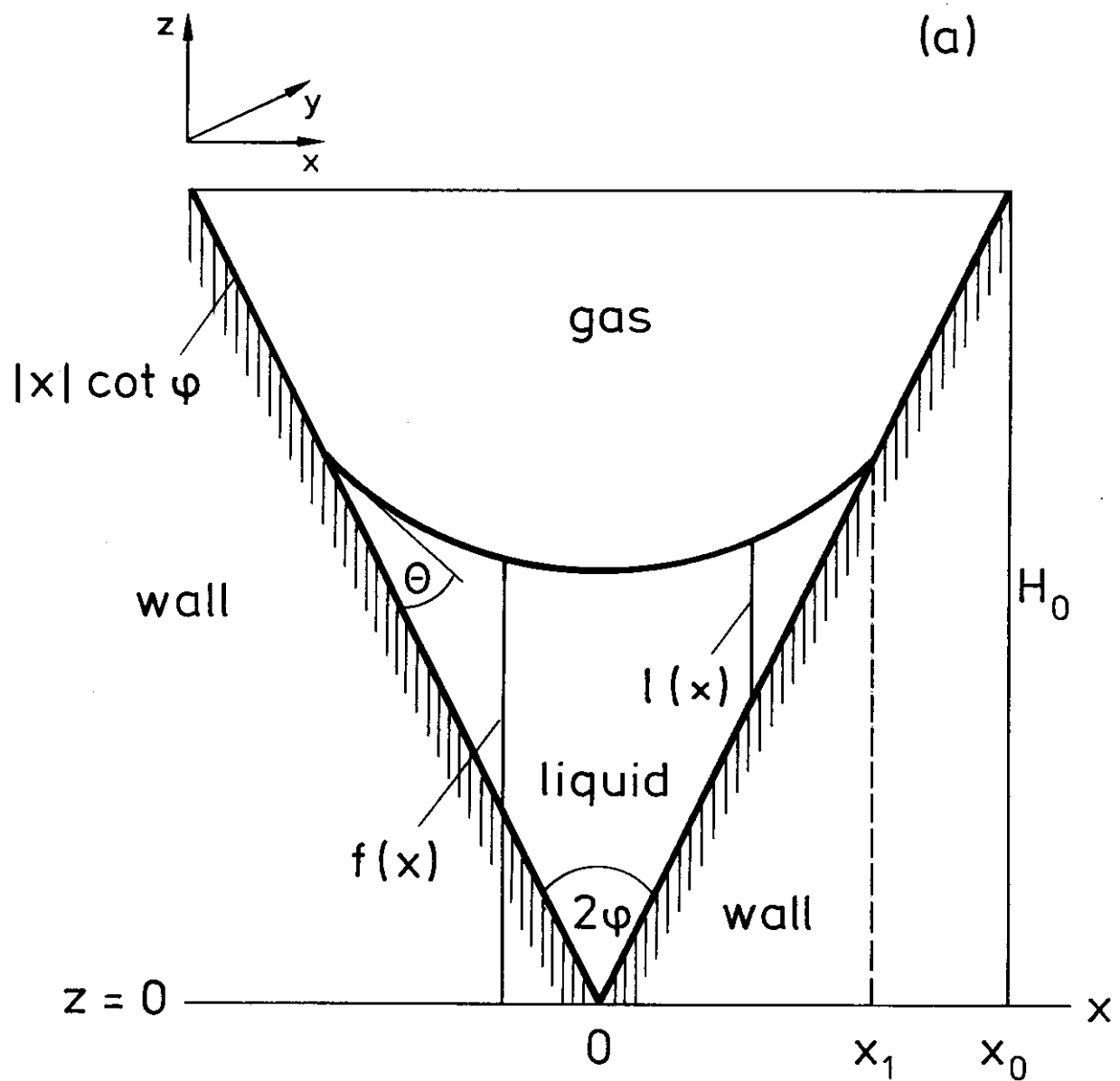


Fig. 1 (a)

(b)

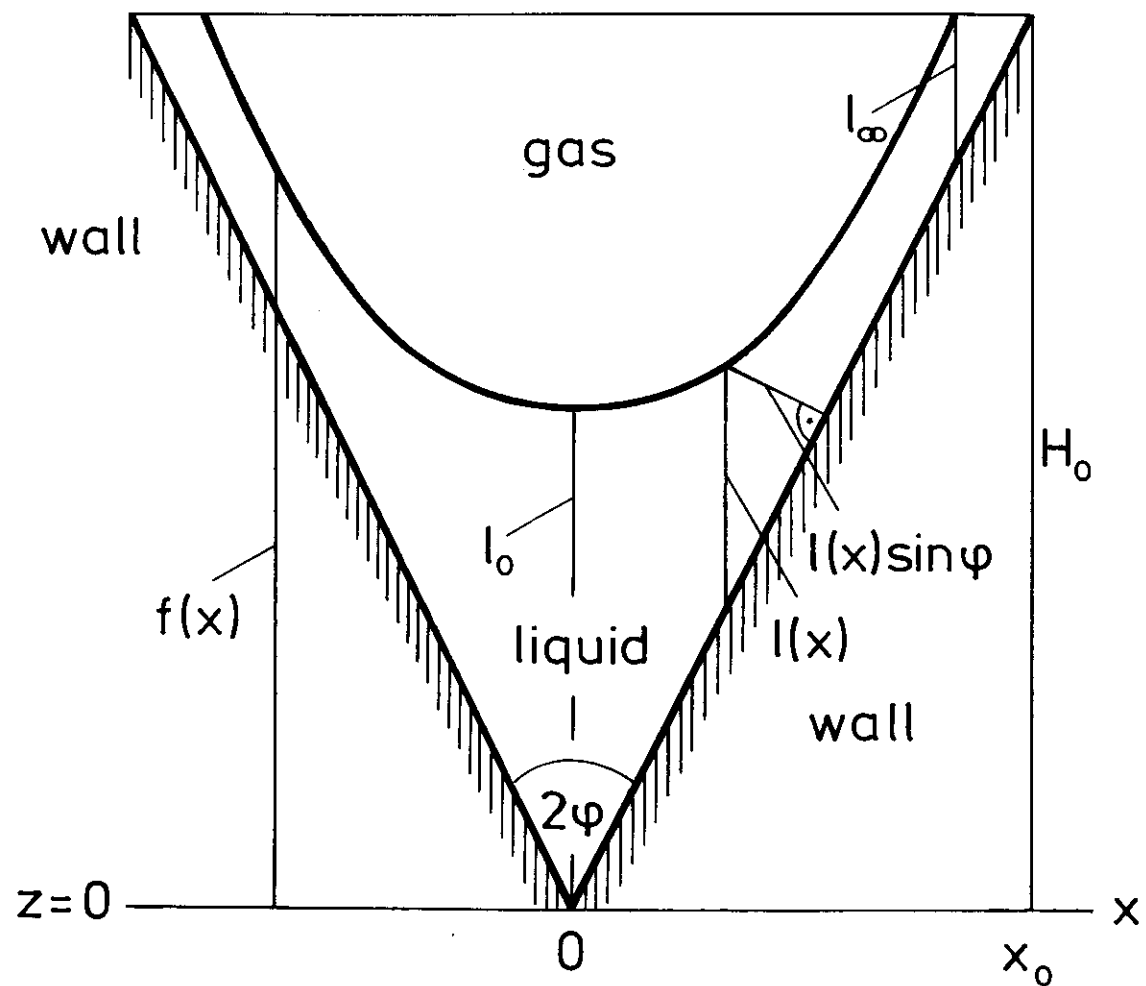
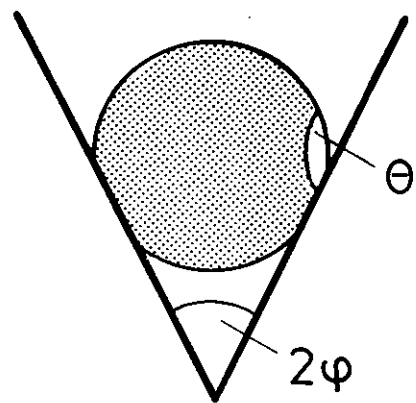
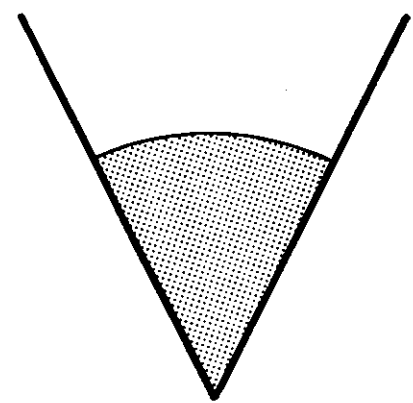


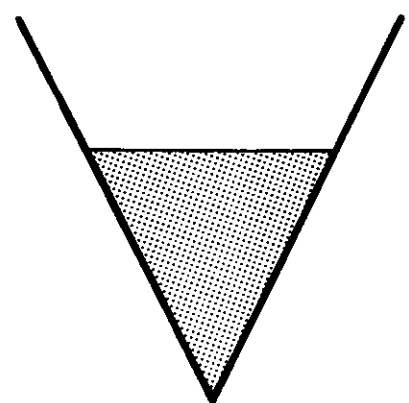
Fig. 1(b)



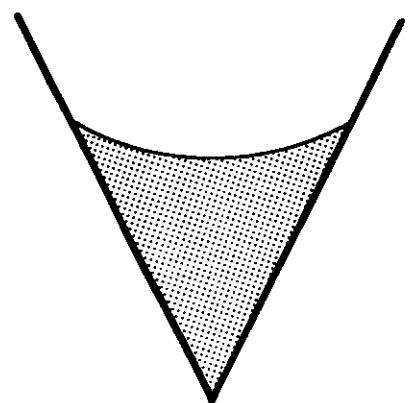
$$\theta > \frac{1}{2}\pi + \varphi$$



$$\frac{1}{2}\pi + \varphi \geq \theta > \frac{1}{2}\pi - \varphi$$



$$\theta = \frac{1}{2}\pi - \varphi$$



$$\theta < \frac{1}{2}\pi - \varphi$$

Fig. 2

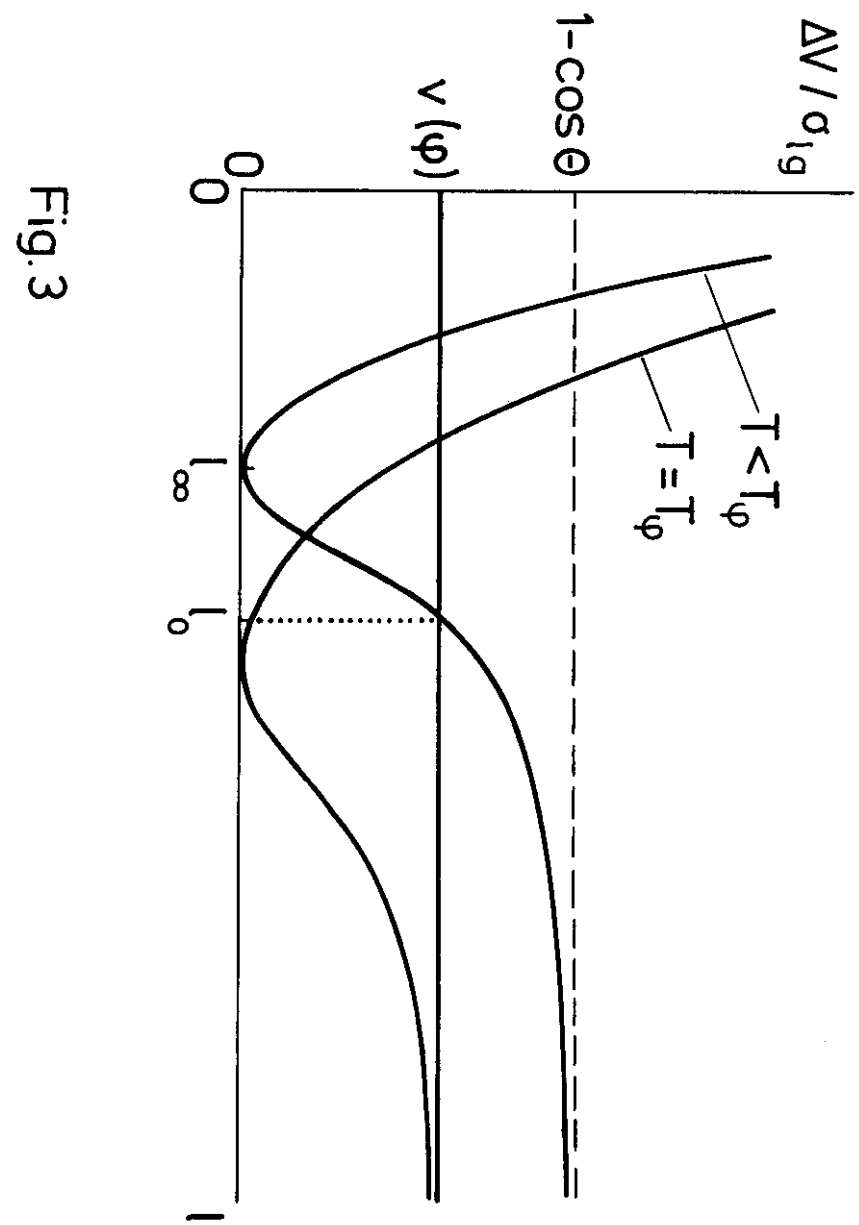


Fig.3

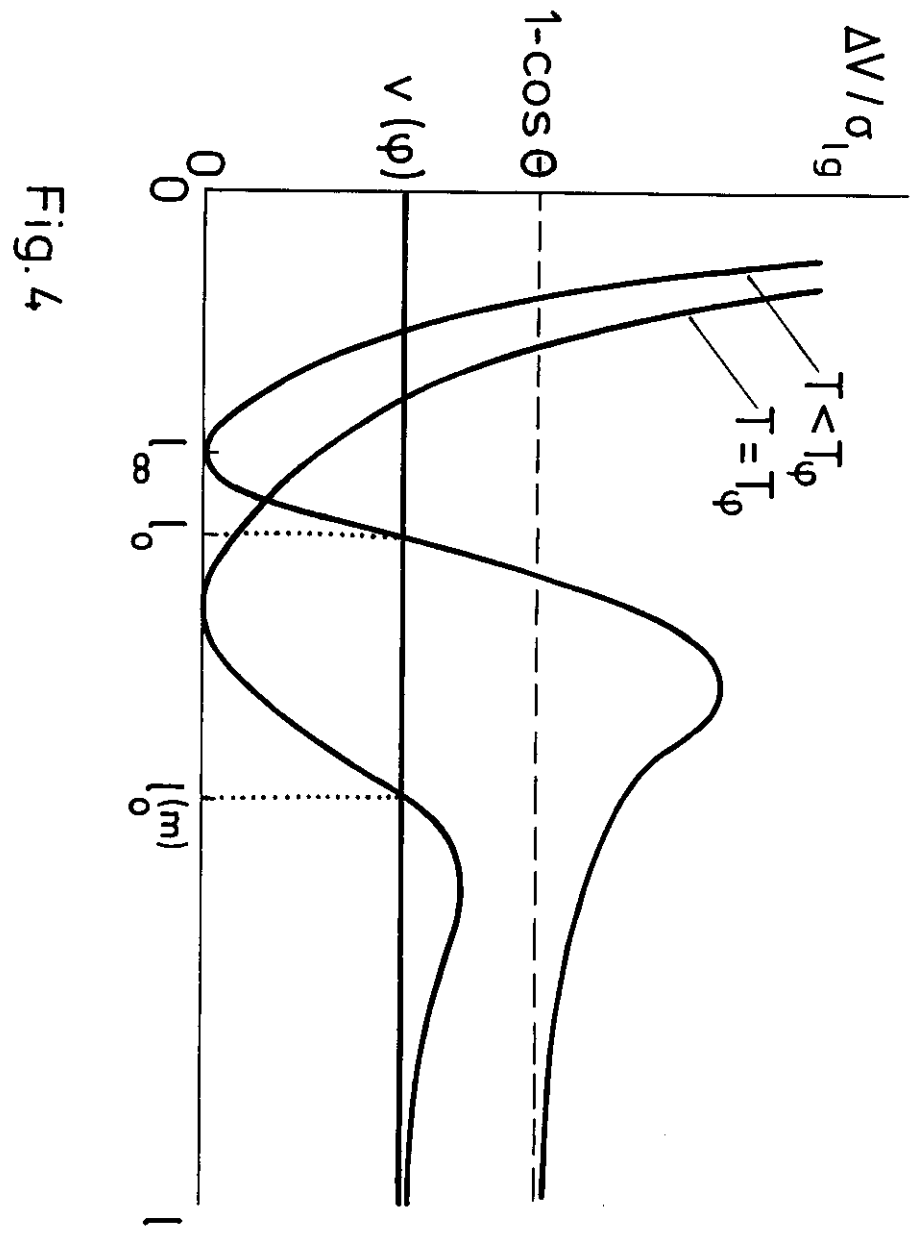


Fig. 4

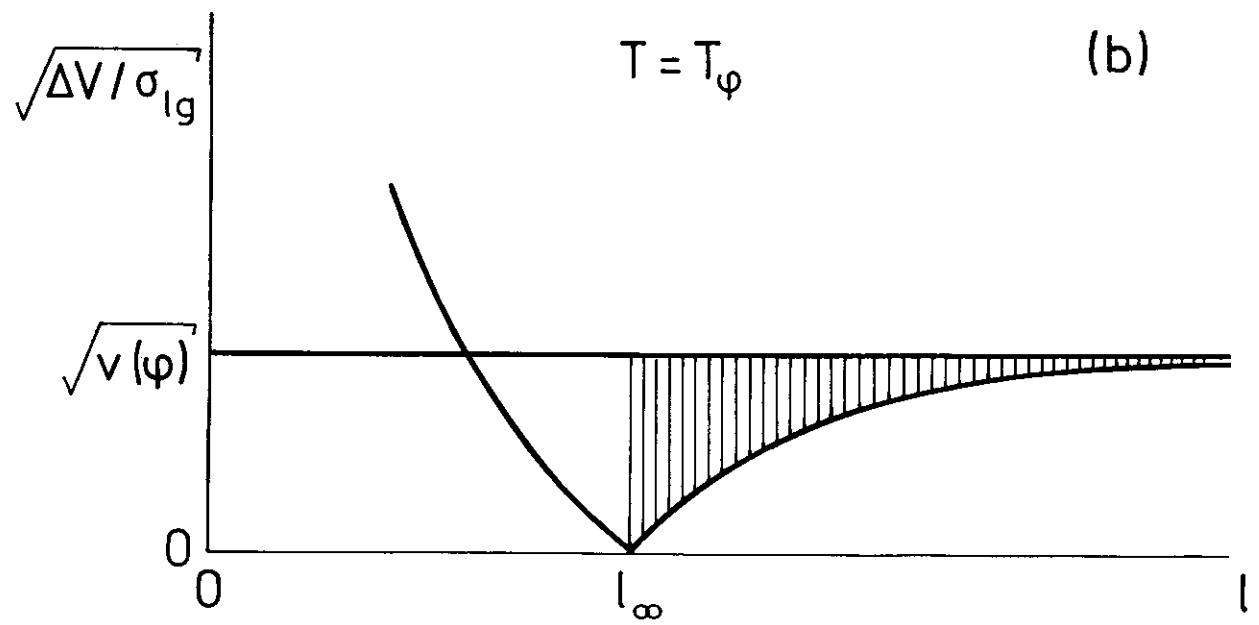
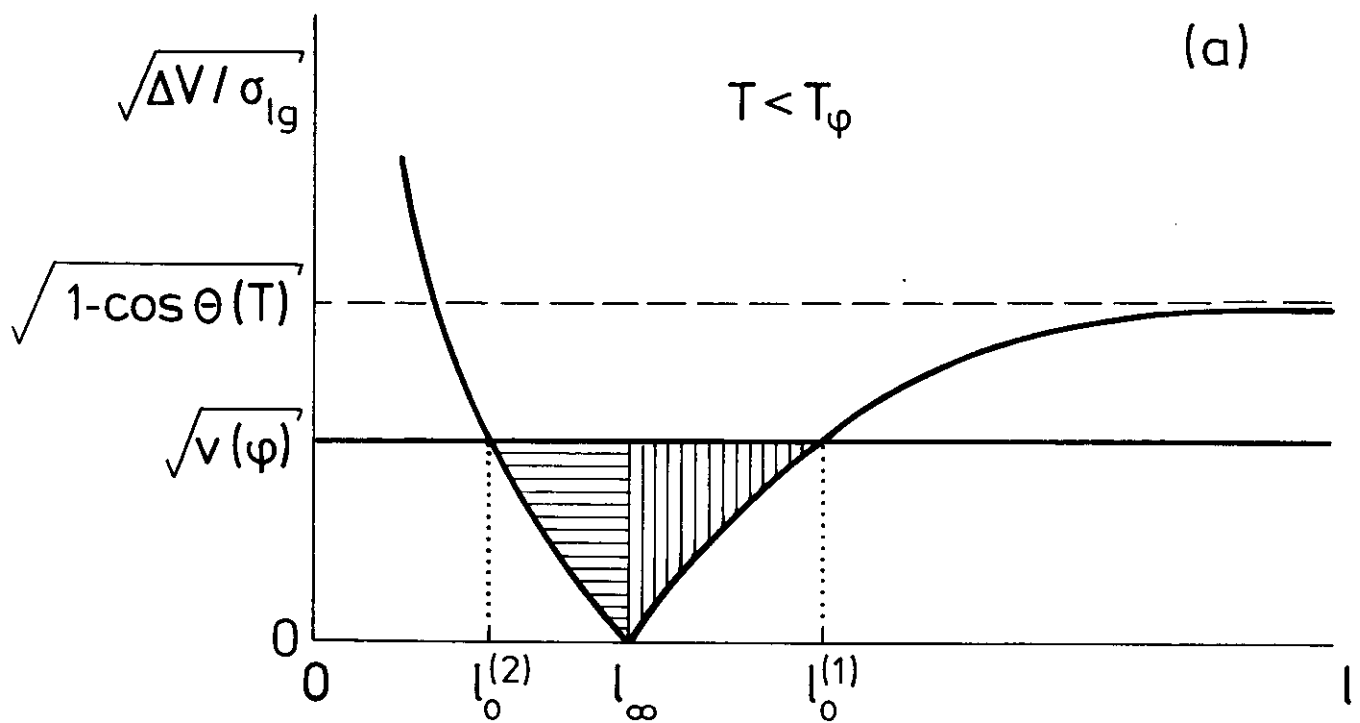


Fig. 5

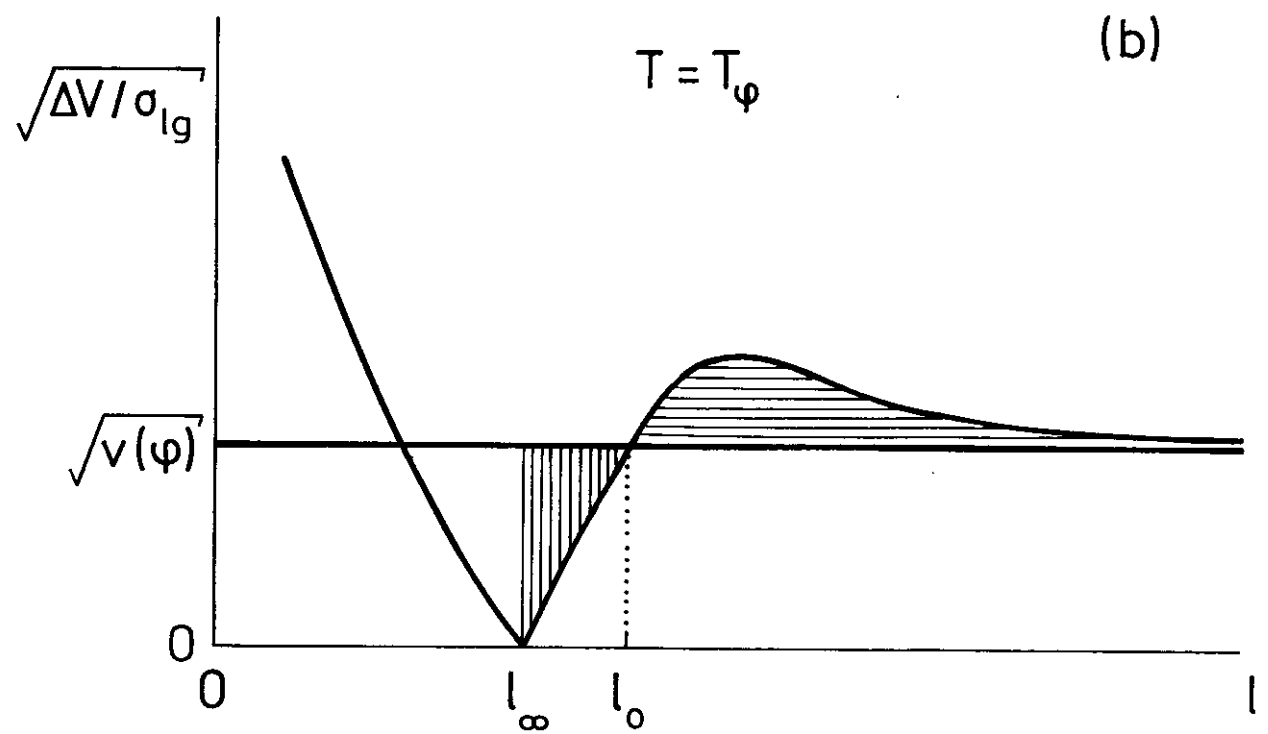
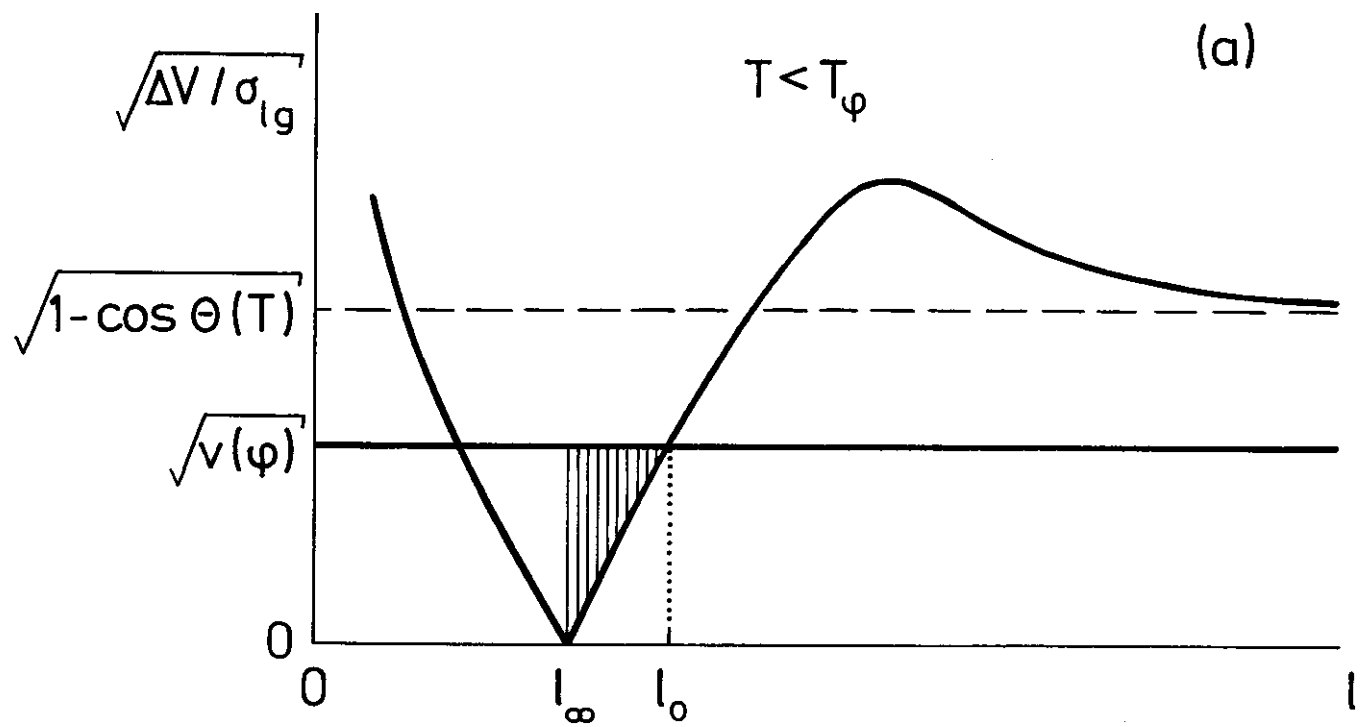


Fig. 6

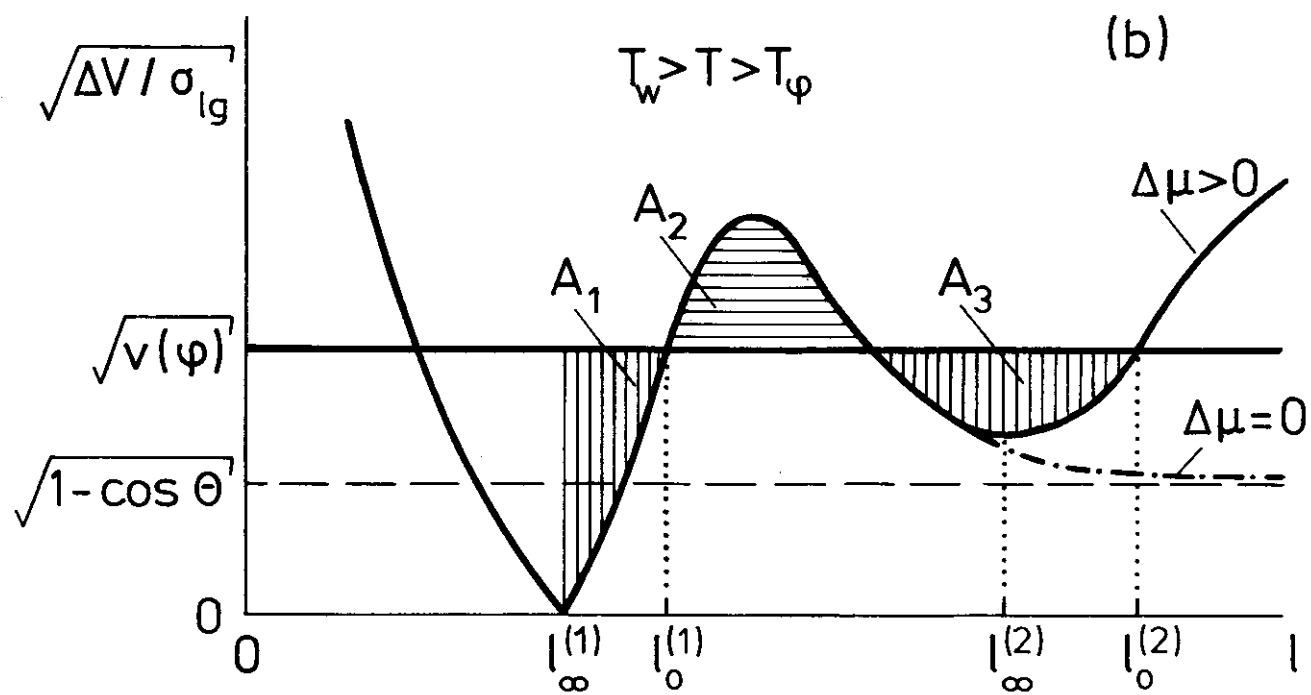
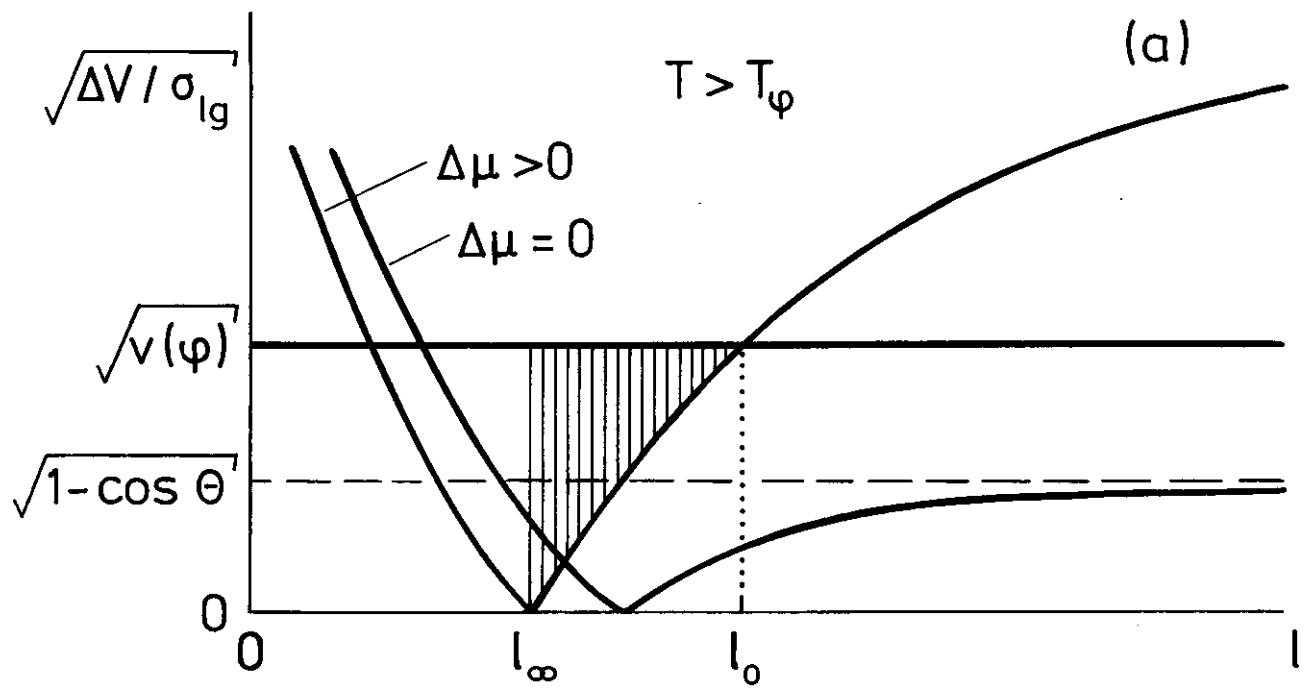


Fig. 7

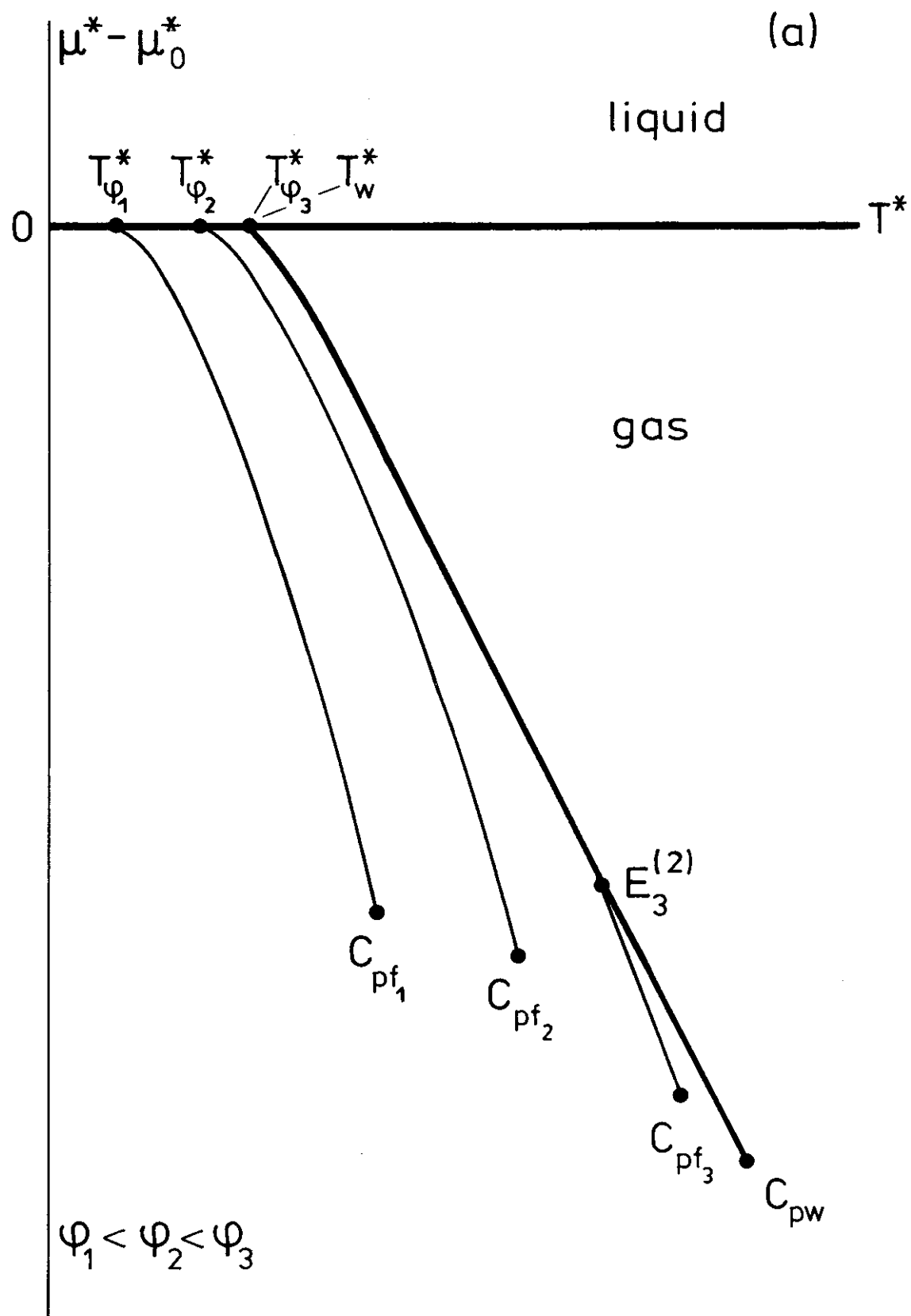


Fig. 8(a)

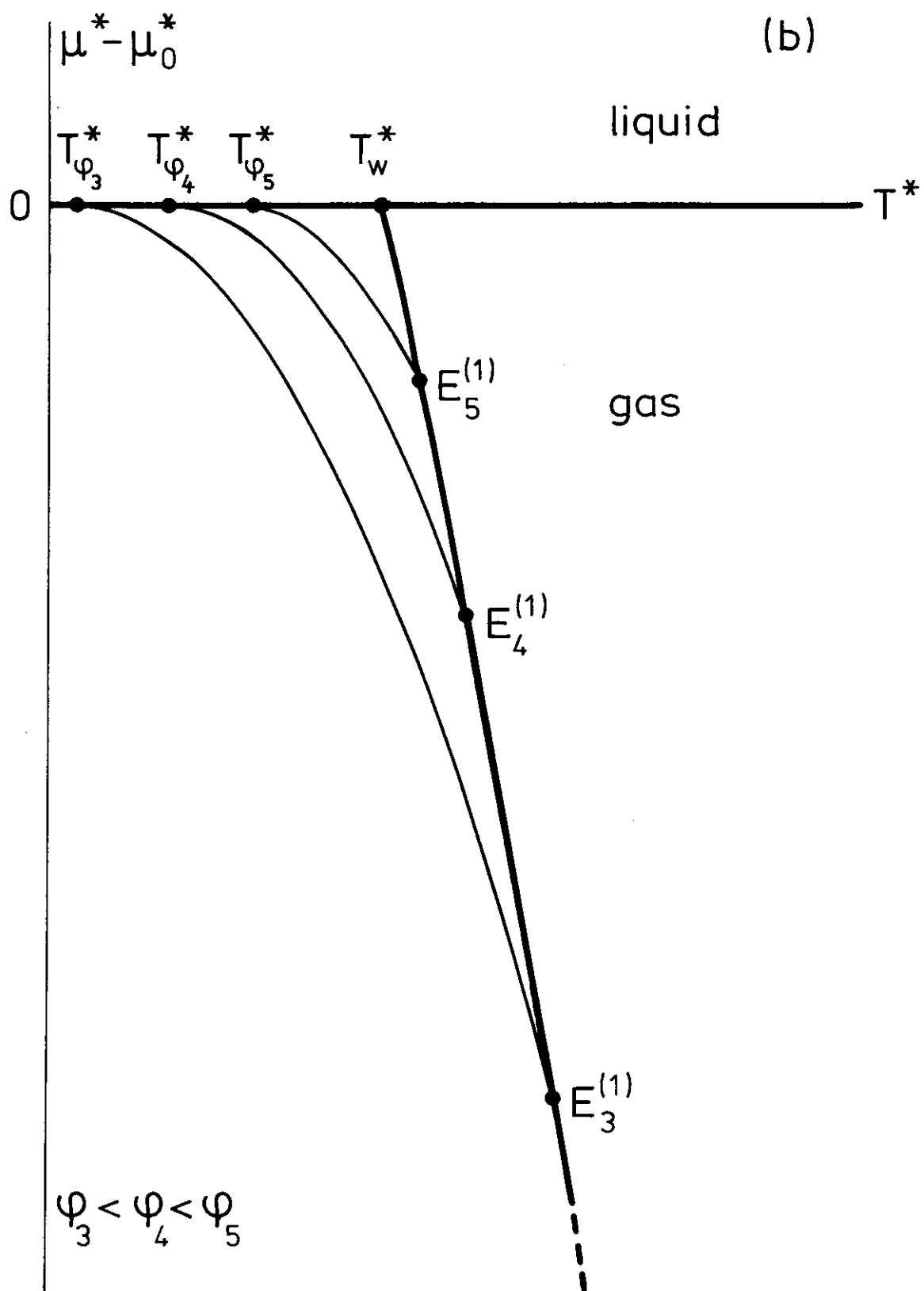


Fig. 8(b)

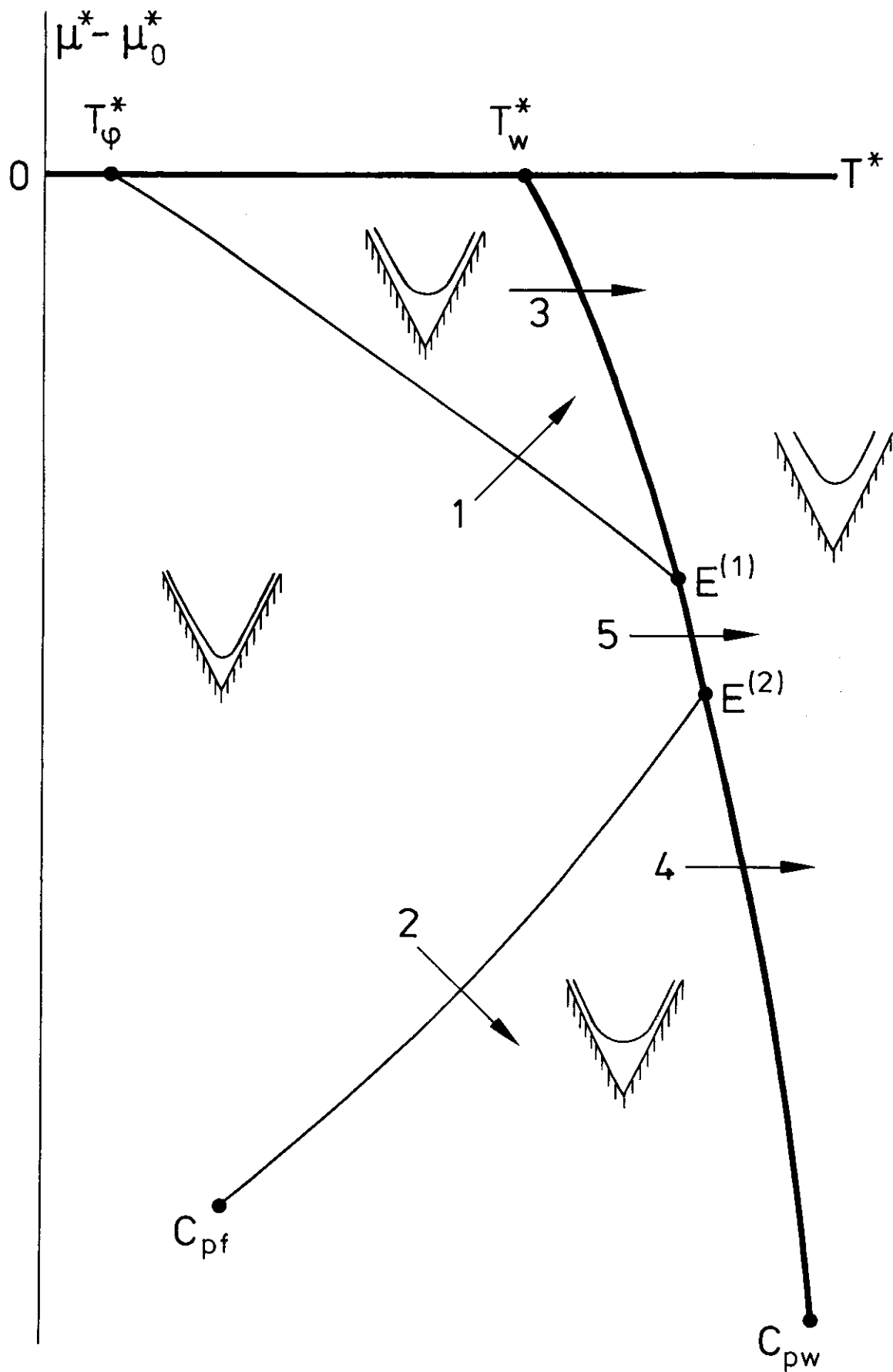


Fig. 9

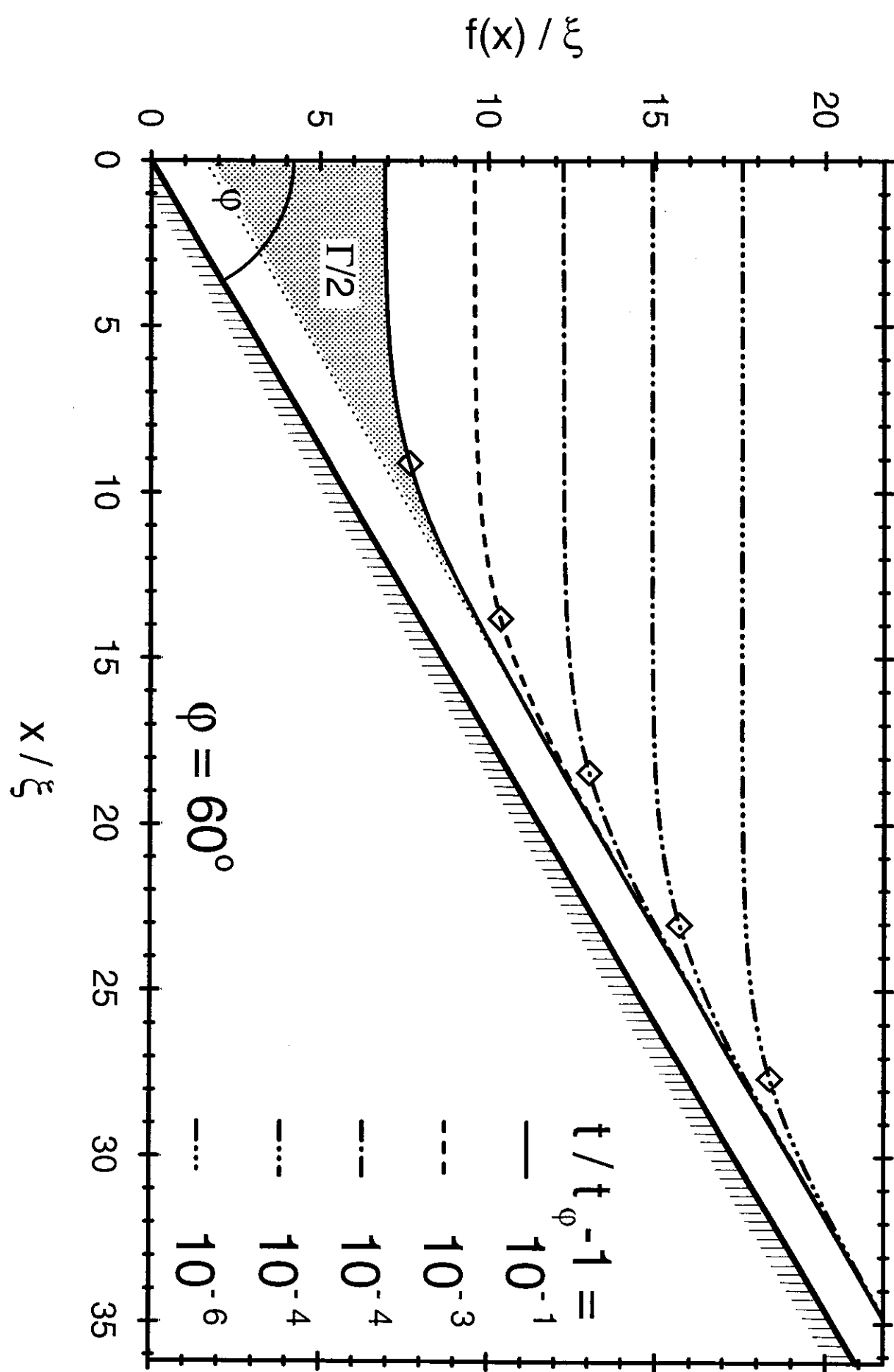


Fig. 10

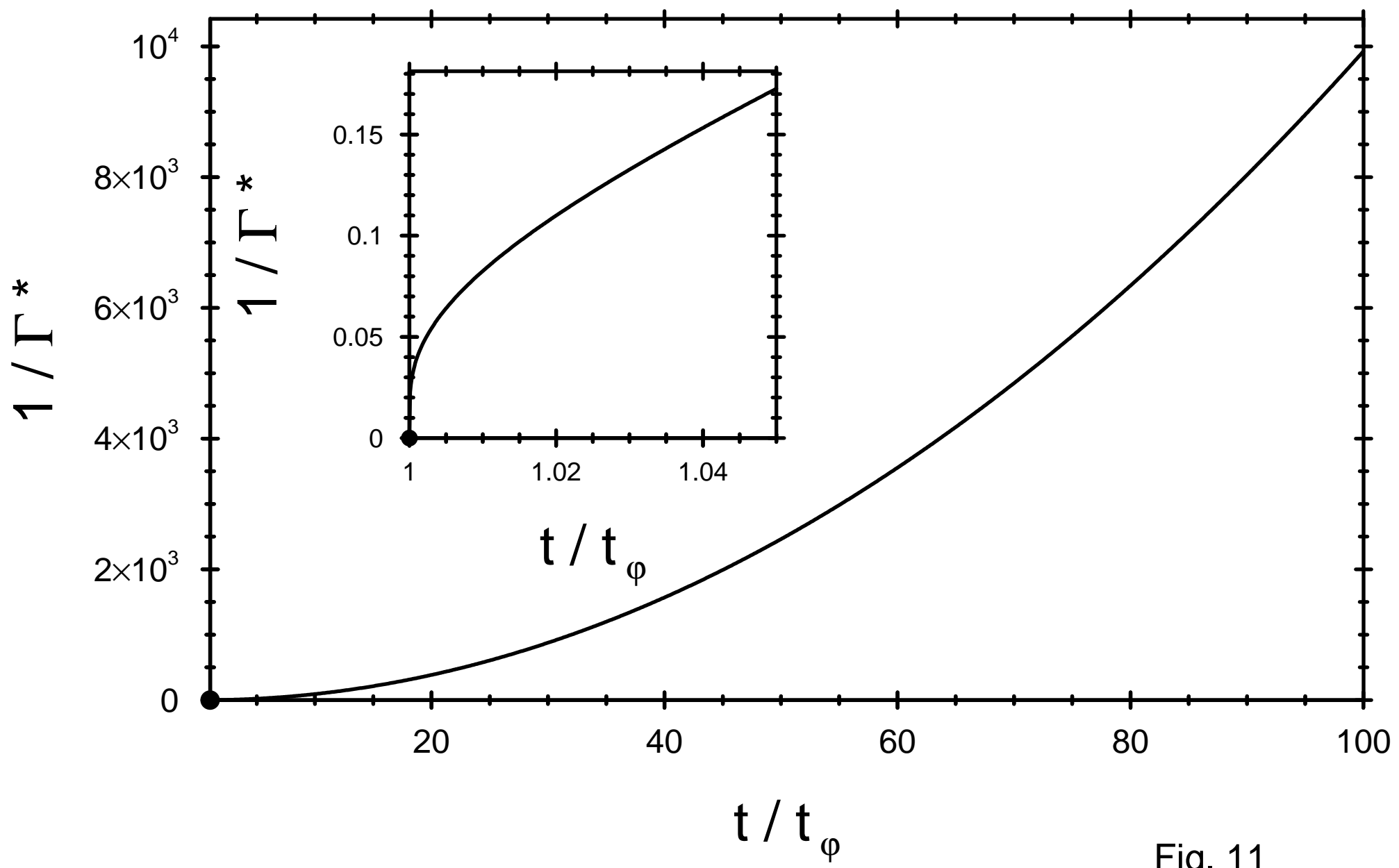


Fig. 11

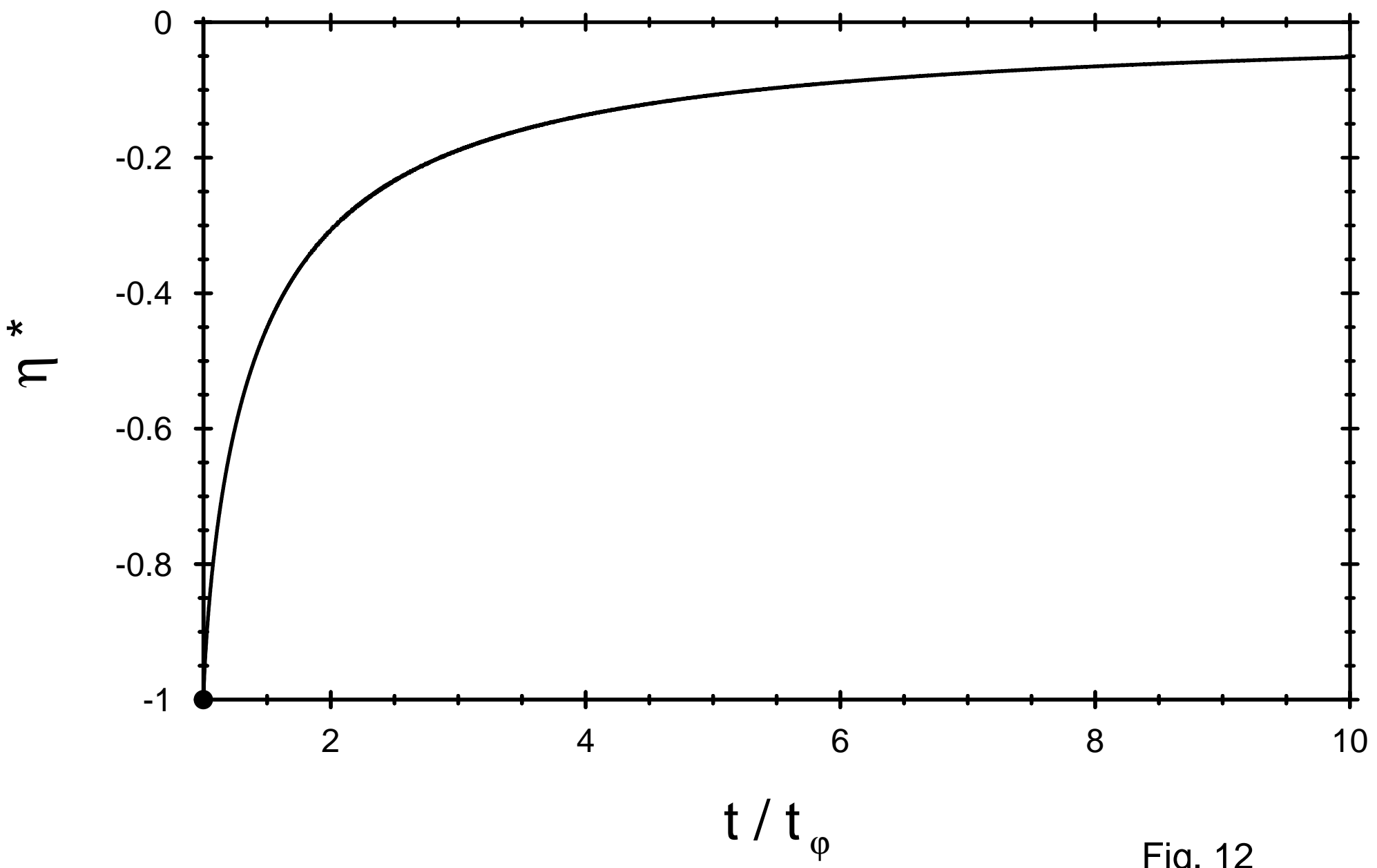


Fig. 12